THE MARINE NITROGEN CYCLE ACROSS THE CRETACEOUS-PALEOGENE BOUNDARY AT MAUD RISE

By

BRADLEY ALAN BECKWITH

Bachelor of Science in Geosciences

Texas Tech University

Lubbock, Texas

2013

Submitted to the Faculty of the
Graduate College of the
Oklahoma State University
in partial fulfillment of
the requirements for
the Degree of
MASTER OF SCIENCE
July, 2016

THE MARINE NITROGEN CYCLE ACROSS THE CRETACEOUS-PALEOGENE BOUNDARY AT MAUD RISE

Thesis Approved:

Dr. Tracy M. Quan

Thesis Adviser

Dr. Eliot A. Atekwana

Dr. Jack C. Pashin

ACKNOWLEDGEMENTS

Dr. Tracy Quan, for developing the proposal to investigate the nitrogen cycle and water column conditions across the K-Pg boundary, funding my graduate education, and providing guidance during this research project. This was truly an interdisciplinary project, and I received broad exposure to all branches of the geosciences during the course of it.

Dr. Eliot Atekwana, for the countless hours he spent with me in the geochemistry laboratory. My time spent in the geochemistry lab will help me to evaluate the quality of the data I use in industry, since I now have a good understanding of how it was collected.

Dr. Jack Pashin, for his invaluable insight during this process, particularly on how to approach my analysis of the data and move forward. He told me, "You can only prove or disprove with the data you have."

Ocean Drilling Program Scientists, for coming together to advance our knowledge of the earth sciences. The previously published studies on Maud Rise and the K-Pg boundary were invaluable during this investigation.

Dr. Madhav Machavaram, for his assistance with sample analyses, detailed explanations of Isotope Ratio Mass Spectrometry theory and literature suggestions that would be invaluable if I were to conduct high-resolution sampling of similar sediments in the future.

Tabitha Schneider, for suggesting me as a possible student to Dr. Tracy Quan.

Name: BRADLEY ALAN BECKWITH

Date of Degree: JULY, 2016

Title of Study: THE MARINE NITROGEN CYCLE ACROSS THE CRETACEOUS-PALEOGENE BOUNDARY AT MAUD RISE

Major Field: GEOLOGY

Abstract:

The marine nitrogen cycle across the Cretaceous-Paleogene (K-Pg) boundary at Maud Rise provides insight into an important environmental variable during the K-Pg extinction event, the redox state of the water column. This is because reactions in the marine nitrogen cycle are redox dependent, and evidence of them is preserved within the organic matter (OM) deposited and buried within the sediments. We evaluated the sedimentary nitrogen stable isotope ratio ($\delta^{15}N$) values across the K-Pg boundary at Maud Rise, a seamount at a high latitude location in the Southern Ocean (65°9.621'S; 1°12.285'E), and can relate the severity and length of recovery period at Maud Rise to variations in the water column redox state. We digested the calcareous ooze core samples recovered from Maud Rise (Ocean Drilling Program Site 690) in 30% HCl to remove carbonate, and then obtained our $\delta^{15}N$ values using an Elemental Analyzer (EA) interfaced to an Isotope Ratio Mass Spectrometer (IRMS). We also collected sedimentary organic carbon stable isotope ratio ($\delta^{13}C_{org}$) values and the elemental concentrations of nitrogen (N) and carbon (C) of the decarbonated sediment fraction with this method. Our $\delta^{15}N$ values indicate that oxic conditions prevailed at Maud Rise through the reddish-brown marl interval of the core following the K-Pg boundary, and that Maud Rise was oxic or suboxic through the Late Cretaceous, early Paleocene and late Paleocene intervals analyzed in this study. Cross-plots of our $\delta^{13}C_{org}$ values and C/N ratios indicate the primary source of OM at Maud Rise was from marine phytoplankton, with some contribution from C3 land plants. The oxic conditions contributed to the more rapid recovery of calcifying plankton at Maud Rise in comparison to mid and low latitude locations, because surviving/existing taxa were already adapted to the oxic water column conditions at Maud Rise, an important environmental variable.

TABLE OF CONTENTS

Chapter Page

LIST OF TABLES

LIST OF FIGURES

CHAPTER I

INTRODUCTION

Motivation behind our Investigation of the Nitrogen Cycle at Maud Rise during the Cretaceous-Paleogene Extinction Event

This investigation seeks to evaluate the changes in the marine nitrogen cycle in order to determine the redox state of the water column across the Cretaceous-Paleogene (K-Pg) boundary at Maud Rise. Maud Rise (Ocean Drilling Program (ODP) Site 690) is an aseismic ridge located in the Weddell Sea of the Southern Ocean, approximately 700 km offshore of Antarctica. Previous studies have shown that shifts in sedimentary nitrogen isotope ($\delta^{15}N$) values indicate changes in the redox state of the water column (Altabet and Francois, 1994; Ganeshram et al., 2002; Quan et al., 2008; Quan and Falkowski, 2009; Sigman et al, 2009; Ryabenko et al., 2012; Quan et al., 2013). Furthermore, this is the first investigation of sedimentary $\delta^{15}N$ values at a high latitude K-Pg boundary site in the Southern hemisphere, which allows us to compare with redox conditions observed across K-Pg boundaries at low and mid latitude locations.

The majority of the scientific community accept that a bolide impact caused the K-Pg extinction event (Alvarez et al., 1980; Smit, 1999; Schulte et al., 2010). The location of the impact crater is near the town of Chicxulub, in the Yucatán Peninsula of Mexico. An increase in iridium (Ir) is associated with the boundary, and is as a primary marker for the K-Pg extinction event in the sedimentary rock record (Alvarez et al., 1980; Michel et al., 1990; Smit, 1999; MacLeod et al., 2007). Other scientists accept that volcanism was a primary mechanism for the extinction event, or an additional environmental stressor leading up to the K-Pg extinction event (Keller, 2003; Keller et al., 2004; Robinson et al., 2009; Renne et al., 2015; Schoene et al., 2015). The K-Pg extinction event devastated calcifying phytoplankton populations in the marine realm, with over 90% of planktonic foraminifera species and calcareous nannoplankton species extinct (Olsson and Liu, 1993; Bown, 2005; D'Hondt, 2005; Bernaola and Monechi, 2007; Jiang et al., 2010). Core 15X of Hole 690C at Maud Rise (ODP Site 690) is a foraminifer bearing muddy nannofossil chalk that contains a continuous K-Pg boundary (Shipboard Scientific Party, 1988b). Therefore, Maud Rise is an excellent location to evaluate changes in the nitrogen cycle and its relationship to the extinction of planktonic foraminifera and calcareous nannofossils.

There are many competing models of the ocean during the K-Pg mass extinction event. There is the "Strangelove Ocean" model, where marine primary productivity is continually suppressed in the oceans of the early Paleocene following the extinction event (Hsü et al., 1982; Hsü and McKenzie, 1985; Arthur and Zachos, 1987; Kump, 1991). Another model suggests marine primary production continued to be high, but the amount of organic flux to the sediments was low in comparison to pre-extinction conditions

(D'Hondt et al., 1998; D'Hondt, 2005). It is referred to as the "Living Ocean" model (Adams et al., 2004). Another competing model is the "Resilient Ocean", related to the lack of benthic foraminifera extinctions during the K-Pg extinction, as the benthic foraminifera required organic matter to be delivered from the surface production in order to survive (Alegret and Thomas, 2009; Alegret and Thomas, 2013). It has been argued that the benthic foraminifera would have been able to survive on flocks of marine snow that were transported to them in the absence of zooplankton disaggregation (Turner, 2002; Alegret et al., 2012). An additional model is the "Heterogeneous Ocean", in which recovery of primary production following the K-Pg extinction event is often spatially heterogeneous and frequently dependent upon local conditions (Hull et al., 2011b; Sibert et al., 2014; Esmeray-Senlet et al., 2015).

The carbon cycle has been extensively studied across the K-Pg boundary. A negative excursion of 2‰ in the stable isotope ratios of inorganic carbon ($\delta^{13}C_{carb}$) following the K-Pg boundary occurs in both marine and terrestrial records, along with a decrease in calcium carbonate concentration. (Boersma and Shackleton, 1981; Hsü and McKenzie, 1985; Arthur et al., 1987; Zachos and Arthur, 1986; Zachos et al., 1989; Corfield, 1994; Francois et al., 1995; D'Hondt et al., 1998; Kaiho et al, 1999). A decrease in the deposition of biogenic barium (Ba_{bio}), which is used as a proxy for organic matter flux to sediments in oxic environments (Dymond et al., 1992; Francois et al., 1995), occurs after the boundary at many K-Pg locations, including Maud Rise Site 690 (Hull and Norris, 2011). A negative excursion in stable isotopes ratios of organic carbon ($\delta^{13}C_{org}$) occurs at multiple marine locations across the K-Pg boundary (Shatsky Rise, New Jersey continental rise, Brazos River, and Moreno Formation) but the excursion

varies by locality in comparison to the $\delta^{13}C_{carb}$ record, and sampling resolution is low at these sites (Meyers and Simoneit, 1990; Meyers, 1992a; Meyers, 1992b). A well-defined negative excursion in $\delta^{13}C_{org}$ occurs within a K-Pg eastern Atlantic shelf section (Caravaca, Spain), along with greater organic carbon burial (Kajiwara and Kaiho, 1992; Kaiho et al., 1999). The negative excursions in both $\delta^{13}C_{carb}$ and $\delta^{13}C_{org}$ indicate a period of decreased primary production in the ocean, or a lack of carbonate export to the sediments (Arthur et al., 1987; D'Hondt et al., 1998; Meyers and Simoneit, 1990; Stott and Kennett, 1990; Kaiho et al, 1999). A less pronounced negative excursion in $\delta^{13}C_{carb}$ occurs at our sampling site, the K-Pg boundary of Maud Rise (Shipboard Scientific Party, 1988b; Stott and Kennett, 1990). Surface water productivity at Maud Rise was not reduced for as long as it was at low latitude subtropical and tropical regions following the K-Pg extinction event (Stott and Kennett, 1990; Keller et al., 1993; Barrera and Keller, 1994). Furthermore, the $\Delta\delta^{13}C$ gradient between planktonic and benthic marine organisms was eliminated at low and mid-latitude locations, and did not fully recover for an estimated 3 million years following the extinction event (Hsü and McKenzie, 1985; Stott and Kennett, 1990; Keller et al., 1993; Barrera and Keller, 1994; D'Hondt et al., 1998). However, the $\Delta\delta^{13}C$ gradient was reduced but not eliminated at Maud Rise, suggesting a more rapid recovery occurred at the high latitude locations in the Southern hemisphere (Hsü and McKenzie, 1985; Stott and Kennett, 1990; Keller et al., 1993; Barrera and Keller, 1994; D'Hondt et al., 1998). The high latitude Southern Ocean was the source of many new planktonic foraminifer species after the K-Pg extinction event (Keller et al., 1993; Jiang et al., 2010). These high latitude planktonic foraminifer

consisted of surviving unspecialized small late Cretaceous species, which would eventually migrate to lower latitudes during the early Danian (Keller et al., 1993).

The numerous investigations of the carbon cycle across the K-Pg boundary suggest that the nitrogen cycle must have changed, as nitrogen is a limiting nutrient during primary production and the redox state of the water column affects it as well (Capone et al., 2008). The marine nitrogen cycle across the K-Pg boundary has only been evaluated in shallow marine sections at Stevns Klint, Denmark (Brisman et al., 2001; Sepúlveda et al., 2009), despite the existence of over 350 known K-Pg boundary sections (Schulte et al., 2010). Previous studies have shown that water column oxygen concentrations control the nitrogen cycle, since nitrogen reactions are redox dependent (Altabet and Francois, 1994; Ganeshram et al., 2002; Quan et al., 2008; Sigman et al, 2009; Ryabenko et al., 2012; Quan et al., 2013). Therefore, an investigation of changes in $\delta^{15}N$ values across the K-Pg would reveal changes in the oxygenation of the marine water column, and lead to a better understanding of the K-Pg extinction event and recovery period.

Problem, Hypothesis and Objective

Changes in the redox state of the water column are an important, yet unknown; variable directly related to environmental stability across the K-Pg boundary. The redox state of the water column across the K-Pg boundary at Maud Rise (high latitude Southern Ocean seamount) had not been evaluated. We hypothesized that the $\delta^{15}N$ values would be lower, indicating that nitrification predominated through the reddish-brown marl interval following the K-Pg boundary at Maud Rise (ODP Hole 690C, Core 15X, Sections 3, 4)

and oxic water column conditions occurred. Following this event, the $\delta^{15}N$ values would be higher as suboxic conditions in the water column returned, indicative of increasing denitrification. In order to evaluate this hypothesis, we analyzed decarbonated sediments from the Maud Rise K-Pg boundary for their $\delta^{15}N$ values.

Study Site and Sampling Interval Background

This investigation used core samples collected at Maud Rise (ODP Site 690, 65°9.621'S; 1°12.285'E), an aseismic ridge located in the Weddell Sea (Figure 1). Maud Rise is a seamount, formed during the middle to late Cretaceous, no later than the Campanian (Shipboard Scientific Party, 1988b). Maud Rise is one of the few topographic highs in the Weddell Sea of the Southern Ocean. Maud Rise is shallow enough to preserve calcareous sediments, and is located around 700 km offshore of East Antarctica. Maud Rise sediments of the Late Cretaceous to late Paleocene contain varying amounts of aeolian sediment input from the mainland of East Antarctica (Kennett and Barker, 1990; Robert and Chamley, 1990; Robert and Maillot, 1990; Ehrmann et al., 1992). Its unique depositional environment preserves the pelagic ocean marine nitrogen cycle record, in comparison to shelf settings, which preserve a mixed marine and terrestrial signal due to processes such as coarse clastic sediment deposition and riverine input. The samples used in our study are from Holes 690B and 690C, at Site 690 of ODP Leg 113 (Shipboard Scientific Party, 1988a). Site 690 was 2914 meters below sea level (mbsl) when the cores were collected in 1988. Cores recovered from Holes at Site 690 have been divided into five major lithological units, and our samples are exclusively from Unit IV, which consists of nannofossil and foraminifera bearing oozes and chalks dated from late Cretaceous to late Paleocene, and include a biostratigraphically complete K-Pg boundary

in Hole 690C (Shipboard Scientific Party, 1988b; Thomas et al., 1990). The K-Pg boundary is located in Hole 690C, Core 15X, Section 4 (247.81/82 mbsf), and is described as being highly bioturbated and pale reddish-brown in color. (Shipboard Scientific Party, 1988b; Pospichal and Wise, 1990; Stott and Kennett, 1990). Maud Rise has had many previous geological investigations to constrain the results of our investigation, including biostratigraphy, stable isotopes, radioactive isotopes, clay mineralogy, and additional geochemical data (Michel et al., 1990; Pospichal and Wise, 1990; Robert and Maillot, 1990; Stott and Kennett, 1990; Thomas, 1990; Thomas et al., 1990; Hull and Norris, 2011; Alegret et al., 2011; Ravizza and VonderHarr, 2012; Alegret and Thomas, 2013).

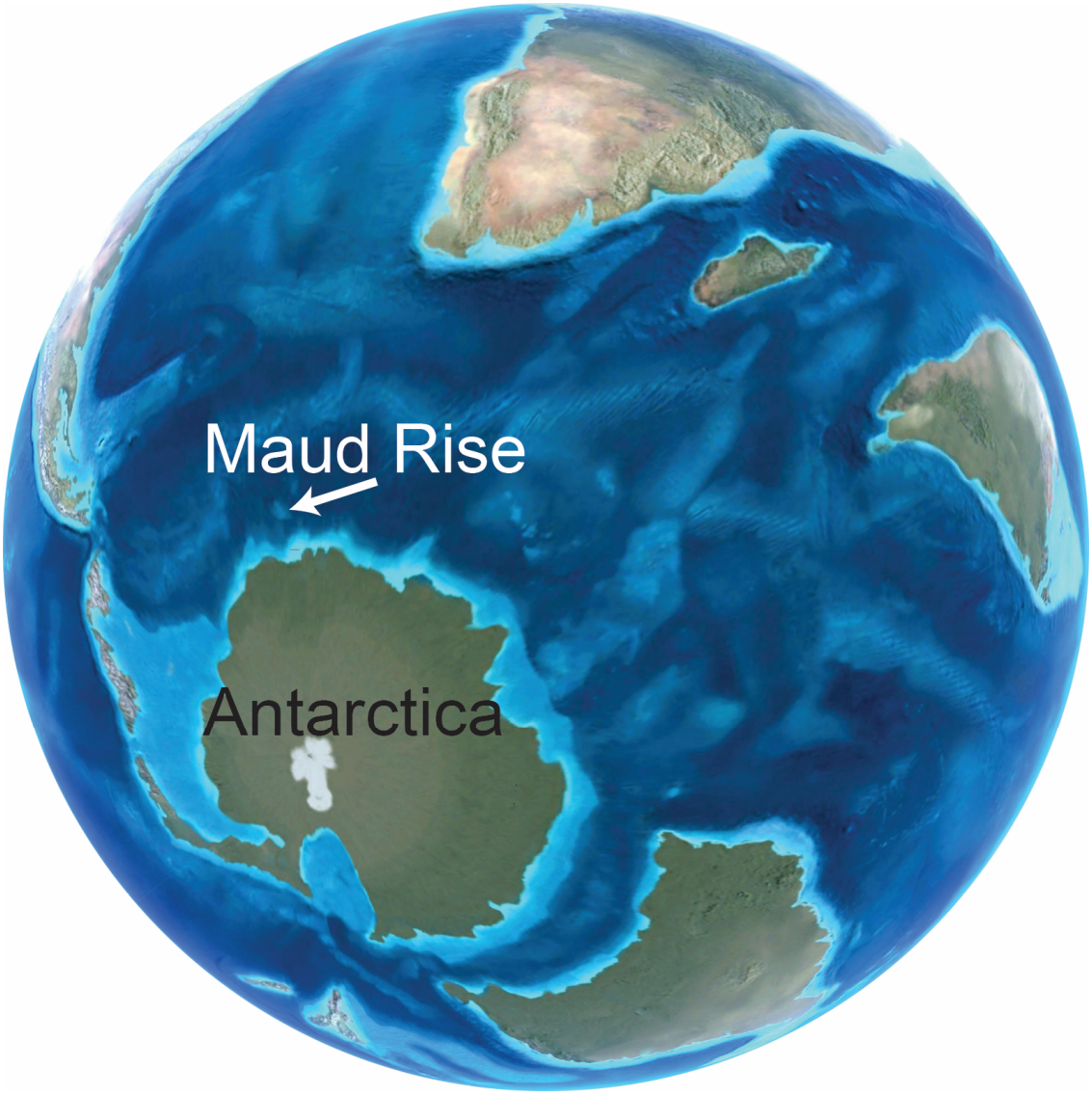

Figure 1. Location of Maud Rise (currently 65°9.621'S; 1°12.285'E) during Cretaceous-Paleogene boundary event, paleogeography map by Blakey (http://cpgeosystems.com)

The Marine Nitrogen Cycle in the Geologic Past

Marine Nitrogen Cycle

The marine nitrogen cycle consists of a variety of redox dependent reactions. Therefore changes in sedimentary $\delta^{15}N$ values, which record predominant surface ocean nitrogen reactions as organic matter (OM) is deposited and buried, are related to changes in oxygen concentrations that previously occurred in the water column (Altabet and Francois, 1994; Capone et al., 2008 and references within; Quan et al., 2008; Sigman et al, 2009; Ryabenko et al., 2012; Quan et al., 2013). Marine organisms utilize various forms of nitrogen, and the nitrogen reactions that occur during utilization are well understood (Wada, 1980; Minagawa and Wada, 1984; Gruber and Galloway, 2008). The four dominant reactions in the nitrogen cycle on geological timescales are nitrogen fixation, nitrification, denitrification and anaerobic ammonium oxidation (anammox) (Figure 2). These reactions each occur different water column oxygen concentrations, and can therefore be used as a paleoredox proxy. These redox controlled reactions change the $\delta^{15}N$ values of the OM, which is preserved if rapid burial occurs (Minagawa and Wada, 1984; Altabet and Francois, 1994). Additionally, OM burial efficiencies in anoxic and oxic depositional environments have been shown to be similar (Thunell et al., 2000). Since the majority of marine OM production is from rapid, high flux events, OM is deposited rapidly to the sediments even in areas of reduced production, and therefore our $\delta^{15}N$ values should be representative of the surface ocean OM $\delta^{15}N$ values (Robinson et al., 2012).

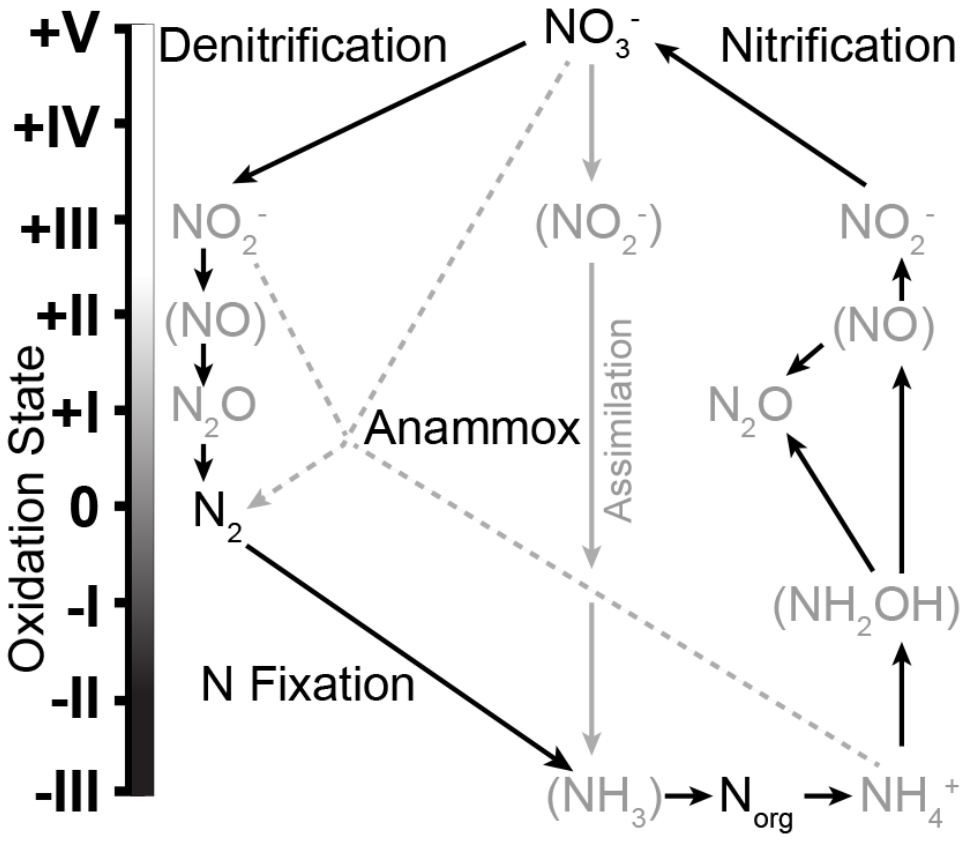

Figure 2. Chemical reactions of nitrogen in the marine realm versus their oxidation state. N fixation, denitrification/anammox, and nitrification are the predominant reactions preserved in the organic matter of sediments on geological timescales (Adapted from Altabet, 2006)

Nitrogen Fixation

Dinitrogen gas (N_2) comprises approximately 80% of the atmosphere. It is the dominant component of dissolved gas in the global ocean. However, very few marine organisms are capable of producing the nitrogenase enzyme that allows them to utilize this form of nitrogen. These nitrogen fixing organisms are predominately cyanobacteria (Capone et al., 1997). The various N_2 fixing organisms produce fixed nitrogen (organic N or ammonium) with low $\delta^{15}N$ values (Minagawa and Wada, 1984; Macko et al., 1987), the average $\delta^{15}N$ values are between -2 and -1‰ (Minagawa and Wada, 1986). Nitrogen

fixation is the predominate nitrogen reaction under anoxic water column conditions, and the characteristic $\delta^{15}N$ values of the reaction are reflected within the buried OM preserved in the sediments, as are the $\delta^{15}N$ values of the other nitrogen reactions (Altabet and Francois, 1994).

Denitrification

Denitrification releases N_2 by way of biologically mediated reactions occurring in the water column. The water column denitrification reaction occurs under suboxic conditions, when nitrate production is supported by increased oxygen concentrations in the water column. However, oxygen concentrations cannot continue to increase, or the compulsory enzymes used to covert nitrate to N_2 gas during denitrification are hindered and oxygen respiration will occur (Codispoti et al., 2001). The denitrification reaction discriminates against the heavier nitrogen isotope, ^{15}N, thus leaving the residual nitrate pool with higher $\delta^{15}N$ values (Miyake and Wada, 1971; Cline and Kaplan, 1975; Altabet et al., 1999). OM produced from this residual pool is has higher $\delta^{15}N$ values, which are preserved in the sedimentary record.

Anammox

The anammox (anaerobic ammonium oxidation) reaction occurs also occurs under suboxic conditions, when ammonium (NH_4^+) is oxidized by the reaction with nitrite (NO_2^-) under anaerobic conditions to produce N_2. This process is carried out by chemosynthetic bacteria (Kuypers et al., 2003, Brunner et al., 2013). Evidence indicates that anammox preferentially removes ^{14}N from the available ammonium, which results in higher $\delta^{15}N$ values of OM produced in the surface waters (Brunner et al., 2013).

However, due to rather recent discovery of anammox pathway (Brunner et al., 2013), it has not been studied in a wide variety of environments in comparison to denitrification; although it is thought to primarily occur in oxygen minimum zones (OMZ).

Nitrification

Nitrification in the ocean occurs under oxic water column conditions. The coupled reactions behind nitrification involve the oxidation of NH_4^+ to NO_2^- and the oxidation of NO_2^- to nitrate (NO_3^-) by multiple varieties of chemosynthetic bacterium (Miyake and Wada, 1971; Mariotti et al., 1981; Gruber and Galloway, 2008). In the upper and mid water column of oligotrophic waters, nitrification usually continues until completion, with minimal NH_4^+ remaining (Capone et al., 2008). Therefore, the nitrification reaction transfers the nitrogen initially present in NH_4^+ into the NO_3^- pool, and $\delta^{15}N$ values are relatively unchanged (Capone et al., 2008). The nitrification reaction, which occurs under oxic water column conditions, produces lower $\delta^{15}N$ values in comparison to suboxic water columns where denitrification and anammox occur (Wada, 1980; Casciotti and Buchwald, 2012).

A Conceptual Model Relating Sedimentary $\delta^{15}N$ Values to Water Column Redox State

Nitrogen fixation, denitrification/anammox, and nitrification predominate under anoxic, suboxic, and oxic water column conditions, respectively. The characteristic $\delta^{15}N$ values of each reaction are preserved in the OM of marine sediments, as long as rapid burial occurs and NO_3^- is completely assimilated (Altabet and Francois, 1994). Since phytoplankton blooms that generate the majority of OM are rapid, high flux events, OM

is deposited and preserved in sediments of relatively lower productivity regions as well (Robinson et al., 2012). Previous studies have related $\delta^{15}N$ values to the paleoredox state of the marine water column (Quan et al., 2008; Quan and Falkowski, 2009; Sigman et al,

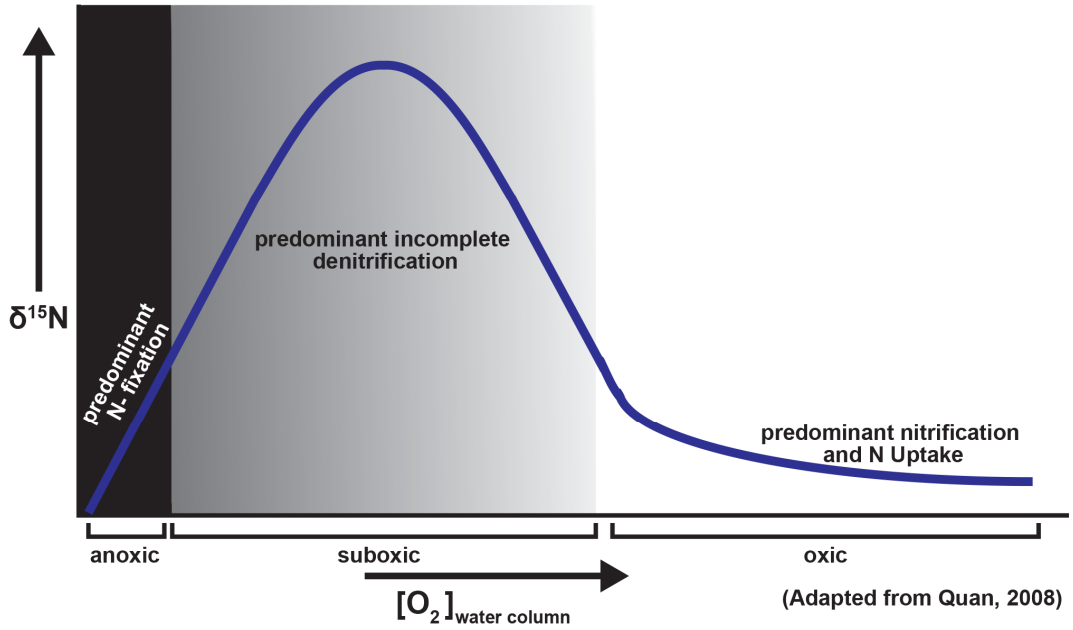

Figure 3. Schematic showing the non-linear relationship between sedimentary $\delta^{15}N$ values and water column oxygen concentrations. Higher $\delta^{15}N$ values are characteristic of the denitrification reaction which predominates under suboxic water column conditions. Lower $\delta^{15}N$ values can indicate either a shift to predominant nitrogen fixation due to an anoxic water column, or predominant nitrification due to an oxygenated water column (Adapted from Quan et al., 2008)

2009; Ryabenko et al., 2012; Quan et al., 2013). Figure 3 is a schematic relating $\delta^{15}N$ values and oxygen concentrations to predominant marine nitrogen cycle reactions and the redox state of the water column. When water column conditions are anoxic, nitrogen fixation by cyanobacteria predominates, this leads to lower sedimentary $\delta^{15}N$ values. When oxygen concentrations start to increase, denitrification begins, in which NO_3^- is converted into N_2, and this reaction favors the lighter nitrogen isotope ^{14}N, leading to higher $\delta^{15}N$ values in the buried sediments. Finally, as oxygen levels continue to increase, then NO_3^- becomes the most stable form of nitrogen in the water column and nitrification

is the predominant reaction. During these periods of increased nitrification, $\delta^{15}N$ values in the organic matter of sediments are lower in comparison to periods of denitrification.

CHAPTER II

METHODS

Sample Collection

We collected bulk sediment samples from the ODP core depository at Texas A&M University, in October of 2012. The cores we selected were from ODP Site 690, located at Maud Rise in the Weddell Sea of the Southern Ocean. The cores were originally retrieved during ODP Leg 113, in January of 1987, at coordinates of 65°9.621'S; 1°12.285'E, and cored to a total sediment depth of 310 meters below sea floor. We initially planned on high resolution sampling every 10 cm through the K-Pg boundary, with lower resolution sampling approximately every 100 cm above and below the boundary. However, we had to adjust our sampling resolution due to lack of continuous core in some of the core sections, since previous researchers had already heavily sampled the cores. We obtained our samples from these cores because their stratigraphic intervals were previously found to contain a complete K-Pg boundary

section, using a combination of biostratigraphy of planktonic foraminifera, benthic foraminifera and calcareous nannofossils, as well as magnetostratigraphy, carbon and oxygen isotope stratigraphy of benthic foraminifers, and calcium carbonate ($CaCO_3$) stratigraphy (Thomas et al., 1990). Hole 690C also contains the iridium anomaly at 247.79 mbsf, which is associated with Chicxulub meteorite impact and the base of the K-Pg boundary (Michel et al., 1990).

Sample Preparation

We crushed and homogenized the bulk sediment samples using a ceramic mortar and pestle, and transferred them to glass sample vials for storage. The sediment samples from Maud Rise often contained high concentrations of $CaCO_3$ (48.40% to 93.80%) through our sampling interval (O'Connell, 1990). Therefore, we digested the homogenized bulk sediments with 30% hydrochloric acid (HCl) in polyethylene centrifuge tubes to remove $CaCO_3$. The $CaCO_3$ free residue was then centrifuged, decanted, and rinsed with deionized water (DI) water. We repeated this process until the decanted solution returned a neutral value of seven on pH paper. We then placed the samples in a laboratory freezer for 12 hours, and then transferred them to a NirTis benchtop K freeze dryer for 24 hours. Next, we crushed and homogenized the freeze-dried sediment samples with a mortar and pestle, and placed them into new glass vials. Unfortunately, we did not record the sample weight prior to decarbonation, and therefore we cannot determine total organic carbon and total nitrogen. All data reported in this thesis are from the decarbonated sediment samples.

Elemental Analyzer and Isotope Ratio Mass Spectrometer Analyses

The decarbonated samples were analyzed for their $\delta^{15}N$ and $\delta^{13}C_{org}$ values, as well as their C and N elemental concentrations using either a Carlo Erba NC 1500 elemental analyzer (EA) coupled with a Thermo Finnigan Delta Plus Isotope Ratio Mass Spectrometer (IRMS) through a Conflo III unit or a CosTech ECS 4010 EA coupled with a Thermo Finnigan Deltaplus XL IRMS. EA oxidation furnace temperature was 1020°C, reduction furnace 750°C, GC oven 50°C, with a He flow rate of 100 mL/min. Dr. Madhav Machavaram (Cincinnati, Ohio) collected the $\delta^{15}N$ values, while $\delta^{13}C_{org}$ values were collected at both Oklahoma State University Geochemistry Laboratory and by Dr. Madhav Machavaram. Samples and standards were loaded into tin capsules prior to combustion. Both labs used CosTech acetanilide for elemental concentrations. Dr. Machavaram used sulfanilamide, ammonium sulfate and in-house lab standard spiders for nitrogen isotopic ratio standards. The spiders were tetragnathids collected from the Little Miami River near Cincinnati, Ohio, which were freeze-dried, powdered and calibrated against NIST standards. Replicates of nitrogen isotopic standards sulfanilamide, ammonium sulfate, and spiders returned standard deviations of ±0.1‰, ± 0.1‰ and 0.3‰. Replicates of organic carbon isotopic standards sucrose (8542) and PE foil (8540) returned standard deviations of ±0.2‰ and ±0.04‰. Replicates of organic carbon isotopic standards USGS 40 and Urea #1 from Oklahoma State University Geochemistry Laboratory returned standard deviations of ±0.1‰ and ±0.1‰**.** Our sample replicates of sedimentary $\delta^{15}N$ values returned a mean standard deviation of ±0.4‰ and a maximum standard deviation of ±0.9‰. Due to large sample size of up to 25 mg, we changed the quartz inserts in the EA after each run.

Reporting of stable isotope ratios

We report isotope ratios using delta (δ) notation with units of per mil (‰):

$$\delta(‰) = \left[\frac{R_{sample}}{R_{standard}} - 1\right] * 1000$$

Where $R_{sample} = {}^{13}C/{}^{12}C_{sample}$ or ${}^{15}N/{}^{14}N_{sample}$ and $R_{standard} = {}^{13}C/{}^{12}C_{\text{Vienna Pee Dee Belemnite (VPDB)}}$ or ${}^{15}N/{}^{14}N_{\text{Atmospheric Nitrogen (Air)}}$

CHAPTER III

RESULTS

Geochemical results: Maud Rise, ODP Site 690 (277.96-192.01 mbsf)

Sedimentary $\delta^{15}N_{decarbonated}$ values range from 1.5 to 12.6‰ with a mean $\delta^{15}N_{decarbonated}$ value of 6 ± 3‰. $\delta^{13}C_{organic}$ values range from -33.5 to -25.2‰ with a mean $\delta^{13}C_{organic}$ value of -27 ± 2‰. C/N (molar) ratios range from 5.4 to 28.0 with a mean ratio of 13 ± 5. See appendices A, B, and C for dataset used in these calculations.

Table 1. Minimum, maximum, average and standard deviation values for $\delta^{15}N_{decarbonated}$ (‰), $\delta^{13}C_{organic}$ (‰), and C/N (molar) ratios of Maud Rise, ODP Site 690 (277.96 – 192.01 mbsf)

	$\delta^{15}N_{decarb}$ (‰)	**$\delta^{13}C_{organic}$ (‰)**	**$C/N_{(molar)}$**
MIN	1.5	-33.5	5.4
MAX	12.6	-25.2	28.0
MEAN	6	-27	13
STDEV	3	2	5

CHAPTER IV

DISCUSSION

The nitrogen cycle and paleoredox conditions across the K-Pg boundary at Maud Rise

The primary focus of this investigation was to investigate the nitrogen cycle and water column conditions across the K-Pg boundary at Maud Rise. However, we collected 99 $\delta^{15}N$ data points from Maud Rise Site 690 (Figure 4) starting at 277.96 mbsf and continuing to 192.01 mbsf. The purpose of this additional sampling was to determine if any longer term changes in the nitrogen cycle occurred. We have divided the data presented in the results section into geochronological time units for the discussion section. The divisions are from Thomas et al. (1990). Our sampling interval was from 277.96 – 192.01 mbsf, this included the Late Cretaceous (277.96 - 247.88 mbsf),

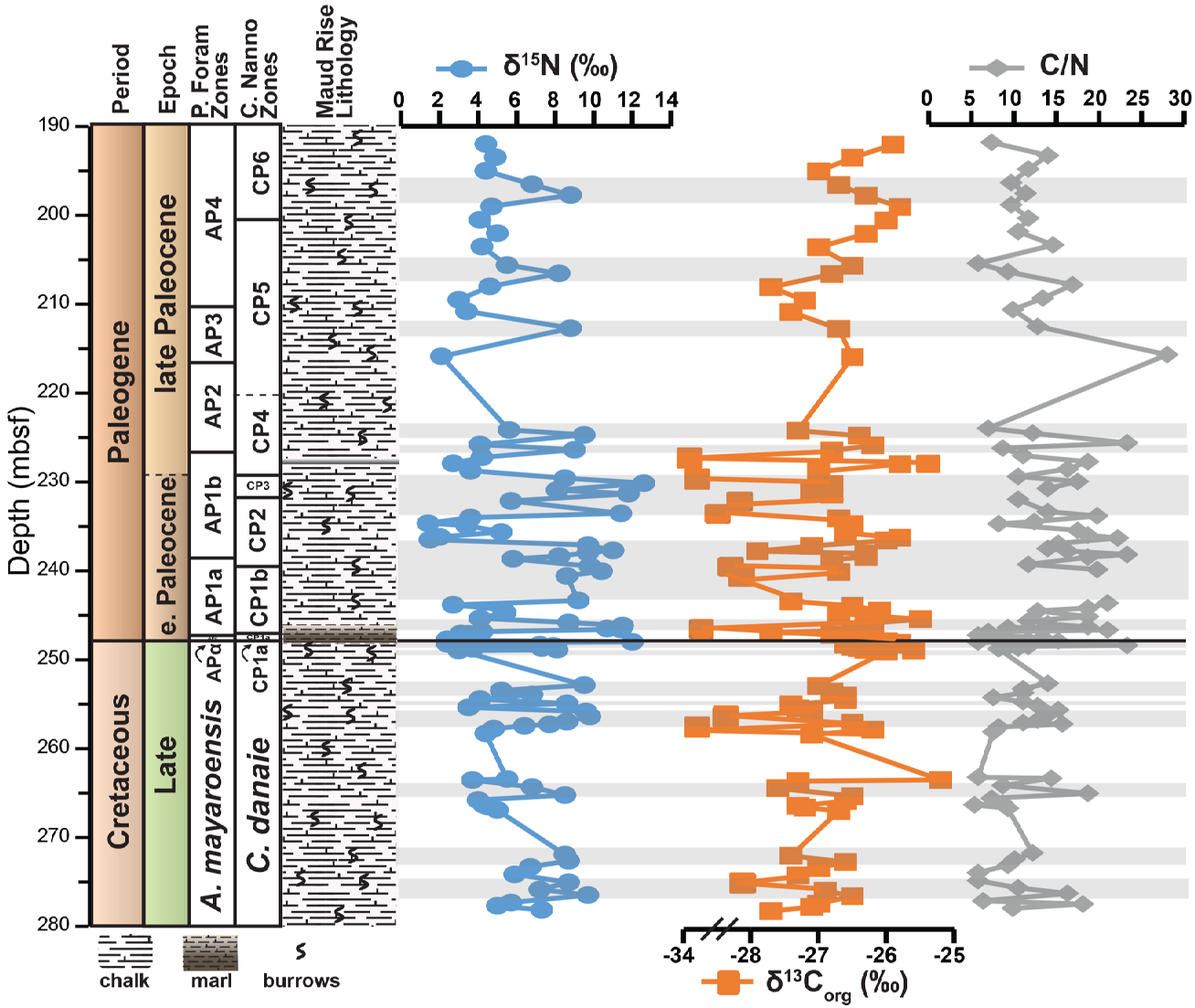

Figure 4. $\delta^{15}N$, $\delta^{13}C_{org}$ and C/N ratios of decarbonated bulk sediment for the Late Cretaceous, reddish-brown Cretaceous-Paleogene boundary marl, early Paleocene and late Paleocene at Maud Rise Site 690, plotted against depth (mbsf), stratigraphic divisions based on the work of Thomas et al. (1990) Note break in $\delta^{13}C_{org}$ values, grey shaded areas represent periods of increasingly suboxic water column conditions, while unshaded areas indicate predominately oxic water column conditions.

Cretaceous-Paleogene boundary reddish brown marl (247.70 - 246.73 mbsf), early Paleocene (264.46 - 230.06 mbsf) and late Paleocene (229.50 - 192.01 mbsf) based on Thomas et al. (1990). These periods have average $\delta^{15}N$ values of 6±2‰, 3±1‰, 8±4‰, and 5±2‰ respectively (Figure 4), therefore the various geological times are statistically the same, and that the nitrogen cycle did not undergo a permanent shift between the Mezozoic and Cenozoic when it is evaluated using those divisions.

The main focus of our investigation was to use $\delta^{15}N$ as a paleoredox indicator across the K-Pg boundary at Maud Rise Site 690. Higher or lower $\delta^{15}N$ values indicate changes in water column oxygen concentrations, with lower $\delta^{15}N$ values and evidence of heavy bioturbation indicative of highly oxic conditions, and shifts toward higher $\delta^{15}N$ values indicating suboxic conditions (Quan et al., 2008; Quan and Falkowski, 2009; Quan et al., 2013). In the reddish brown marl interval (247.7 – 246.73 mbsf) following the K-Pg boundary at Maud Rise (Figure 5), the $\delta^{15}N$ values have the lowest maximum and mean of all the divisions in the core (4.2‰ and 3±1‰). Nitrification is the predominant nitrogen reaction occurring in the water column during this interval, this indicates an oxic water column following the K-Pg boundary at Maud Rise Site 690. We determined this from the low mean $\delta^{15}N$ values (3±1‰) in combination with other geological evidence including intense bioturbation (Pospichal and Wise, 1990), benthic foraminifera species that do not tolerate low oxygen conditions (Thomas, 1990; Alegret and Thomas, 2013), and the reddish-brown boundary layer (Shipboard Scientific Party, 1988b; Hull and Norris, 2011; Hull et al., 2011a). There is a major reduction in calcium carbonate concentrations (O Connell, 1990; Alegret and Thomas, 2013), yet well

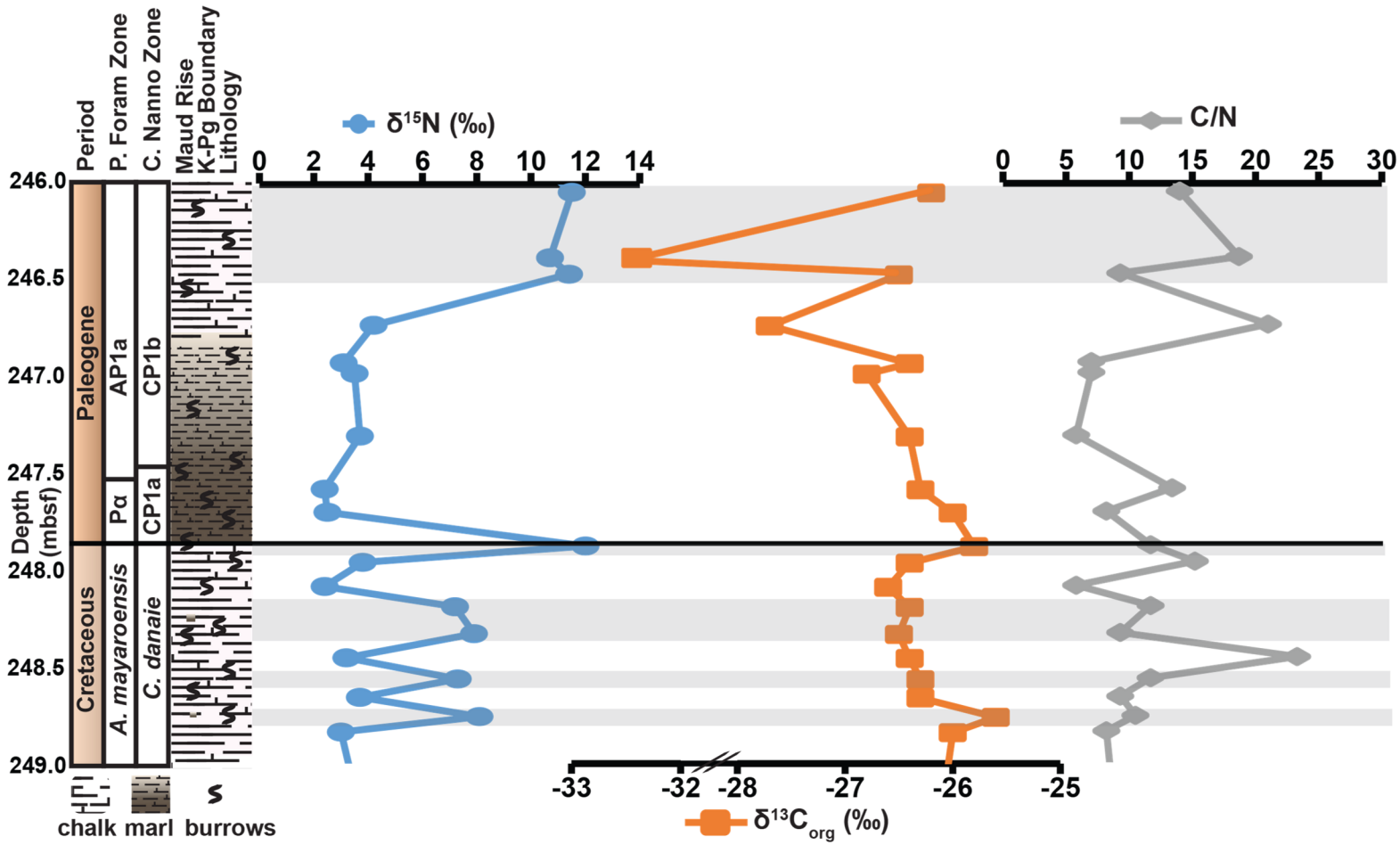

Figure 5. $\delta^{15}N$ values, $\delta^{13}C_{org}$ values and C/N ratios of decarbonated bulk sediment across the Cretaceous - Paleogene boundary at Maud Rise Site 690, plotted against depth, stratigraphic divisions based on the work of Thomas et al. (1990), note break in $\delta^{13}C_{org}$ values, grey shaded areas represent periods of increasingly suboxic water column conditions, while unshaded areas indicate increasingly oxic water column conditions.

preserved calcareous microfossils (Stott and Kennett, 1990) indicating reduced calcifying plankton production, following the K-Pg boundary at Maud Rise Site 690, and a distinct reddish brown color change observed within the core (Shipboard Scientific Party, 1988b; Hull et al., 2011a). Additionally, a negative excursion of 1.8‰ occurs in our $\delta^{13}C_{org}$ isotopes during this interval (Figure 5), indicative of a decrease or lack of export productivity from the surface waters, indicating a reduction or cessation of marine production and a disruption of the ocean's biological carbon pump (D'Hondt, 2005; Schulte et al., 2010). A negative excursion in the $\delta^{13}C$ values of planktonic foraminifers' tests also occurs through the reddish brown marl interval, suggesting a decrease in carbon export and/or burial at Maud Rise (Stott and Kennett, 1989; Stott and Kennett, 1990). The planktonic foraminifera tests through the reddish brown interval are well preserved, with no visible recrystallization (Stott and Kennett, 1990), therefore dissolution of carbonate is not suspected. Additional supporting evidence for a decrease in organic carbon export through the reddish/brown marl interval includes a decrease in biogenic barium deposition (Hull and Norris, 2011), a paleo productivity indicator in oxic depositional environments with minimal terrestrial input (Dymond et al., 1992; Francois et al., 1995). Biogenic barium forms from decaying OM of marine organisms, and Ba deposited in sediments represents dissolution and oxidation of both hard and soft parts of carbonate and siliceous marine organisms from the surface ocean (Dymond, 1981). Furthermore, our C/N (atomic) ratios do not greatly increase beyond the range typical of marine phytoplankton through the reddish brown marl interval, which suggests that input of OM from aeolian terrestrial sources, such as C3 plants, did not increase relative to the other intervals of the core (Figure 5). It is important to note that our higher $\delta^{15}N$ value

directly preceding the K-Pg boundary (247.88 mbsf) indicates increased denitrification at that time, and a shift towards suboxic water column conditions at that point. Due to excellent stratigraphic control through the K-Pg boundary event at Maud Rise (Thomas et al., 1990), we can correlate this $\delta^{15}N$ value to the latest Cretaceous marine transgression (Haq et al., 1987; Haq, 2014). Others have suggested the importance of this sea level high stand as an environmental stressor preceding the K-Pg boundary (Stott and Kennett, 1990; Zachos et al., 1989). This period of increased denitrification provides additional supporting evidence of a major event preceding the boundary observed by Stott and Kennett (1989, 1990), who noted a positive shift in $\delta^{13}C_{carb}$ values of multiple planktonic foraminifera species at Maud Rise during this time.

It is possible to divide our data by periods of oxic and suboxic conditions, as we have done using the grey shading over $\delta^{15}N$ values in both Figure 4 and Figure 5. The grey shaded areas represent higher $\delta^{15}N$ values indicative of suboxic conditions. We would caution against making the statement that Maud Rise had a particular number of oxic or suboxic periods, since sampling resolution was reduced away from the K-Pg boundary. Still, our data indicate that suboxic water column conditions can occur in the pelagic ocean, far from land.

We were curious to see if any changes in the nitrogen cycle might occur along with changing biozonations, however, no clear relationship is apparent at this time (Figure 4). Many of the calcareous nannofossil zones (Pospichal and Wise, 1990) begin with oxic conditions and end during suboxic conditions in the early Paleocene, but this is not true in all cases (Figure 4). Additionally, the rate of change in calcareous nannofossil zones (Pospichal and Wise, 1990) appears to be associated with a greater range of $\delta^{15}N$

values (Figure 4). Still, this is qualitative comparison, as data for each parameter was not collected from the same exact sampling depth in the core (Figure 4).

There are only two published studies of the marine nitrogen cycle across the K-Pg boundary for us to compare our findings with, despite the existence of over 350 known K-Pg boundary sections (Schulte et al., 2010). Those studies investigated shallow marine sections at Stevns Klint, Denmark (Brisman et al., 2001; Sepúlveda et al., 2009). Brisman et al. (2001) analyzed bulk sediment samples for their $\delta^{15}N$ and $\delta^{13}C_{org}$ values across the K-Pg boundary in a shallow marine sequence from Stevns Klint, Denmark. Unfortunately, Brisman et al. (2001) did not utilize biostratigraphic correlation will would allow for better correlation to Maud Rise Site 690. The Stevns Klint section evaluated by Brisman et al. (2001) had lower $\delta^{15}N$ values immediately following the K-Pg boundary, which were about 3.3‰ lower than the rest of their sampling interval. The authors attributed these lower $\delta^{15}N$ values to changes in productivity or lithology (Shemesh et al., 1993; Brisman et al., 2001). We interpret the lower $\delta^{15}N$ values at Stevns Klint to indicate a period of increased nitrogen fixation since it included increased greater carbon burial (higher TOC) associated with anoxic water column conditions. This suggests regional or local variations in the nitrogen cycle across the K-Pg boundary, with low and mid-latitudes experiencing anoxia related to the consequences of the Chixculub impact in the northern hemisphere (Kaiho et al., 1999; Sepulveda et al., 2009; Jiang et al., 2010; Kaiho et al., 2016). In contrast to the low and mid-latitudes, Maud Rise in the Southern Ocean remained oxic throughout the extinction event (Figure 5). Sepúlveda et al. (2009) analyzed $\delta^{15}N$ of kerogen across the K-Pg boundary at Kulstirenden, Stevns Klint, Denmark. Sepúlveda et al. (2009) found evidence that primary productivity of

algae was briefly suppressed, and during this time, the $\delta^{15}N$ and $\delta^{13}C$ values of kerogen were the lowest observed in their investigation, similar to the negative excursion in $\delta^{13}C_{carb}$ values that has been reported globally. Sepúlveda et al. (2009) suggest the post meteorite impact caused these excursions, through the shut down and early recovery stages of primary production at this location. Sepúlveda et al. (2009) conclude bottom waters were depleted of oxygen through this interval, and therefore nitrate depletion through denitrification occurred (Sepúlveda et al., 2009). This stands in contrast to our Maud Rise $\delta^{15}N$ data and depositional environment conditions, which indicate a prolonged period of increased nitrification following the K-Pg boundary at Maud Rise Site 690 (Figure 5), indicating that oxygen concentrations in the high latitude, southern hemisphere, Southern Ocean water column were quite different from the mid latitude, northern hemisphere, Atlantic Ocean water column.

The carbon cycle across the K-Pg boundary at Maud Rise

Cross plots of $\delta^{13}C_{org}$ values and C/N (atomic) are useful during the identification of sedimentary OM sources (Meyers, 1994; Lamb et al., 2006). Our cross plot of the Maud Rise $\delta^{13}C_{org}$ and C/N (atomic) (Figure 6) is from de-carbonated sediments, which could cause slight variations in elemental concentrations related to the acidification process (Kennedy et al., 2005). We plotted our data against datasets complied by Meyers (1994) and our compilation of datasets from modern day Antarctic phytoplankton data (Wada et al., 1987; Biggs et al., 1988), those datasets are shown as grey shaded boxes in figure 6. We find that the sedimentary OM originated primarily from marine phytoplankton, with possible minimal contribution from C3 land plants throughout the Late Cretaceous, Cretaceous-Paleogene boundary marl, early Paleocene and late

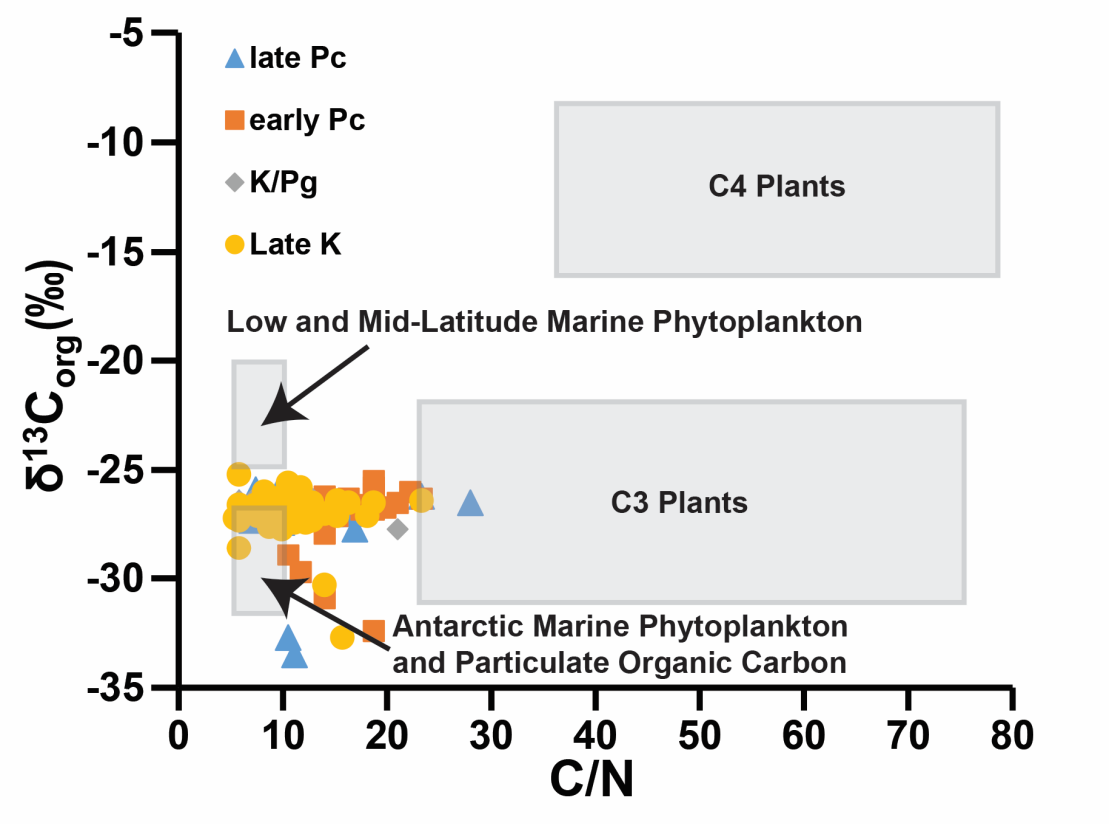

Figure 6. $\delta^{13}C_{org}$ values and C/N ratios of decarbonated bulk sediment for the Late Cretaceous (Late K), Cretaceous/Paleogene boundary marl (K/Pg), early Paleocene (early Pc) and late Paleocene (late Pc) at Maud Rise Site 690, Grey shaded boxes represent data compiled by Meyers (1994), as well as our compilation of Antarctic phytoplankton data from Wada et al. (1987) and Biggs et al. (1988). Maud Rise OM appears to be primarily marine phytoplankton with some input from C3 land plants. These data suggest that the source of OM did not change significantly through the Late Cretaceous into the late Paleocene at Maud Rise.

Paleocene (Figure 6). This implies that source of OM at Maud Rise did not change significantly from the Late Cretaceous into the late Paleocene. Additionally, $\delta^{13}C_{org}$ values and C/N ratios indicate primarily marine production through the reddish-brown marl interval following the K-Pg boundary at Maud Rise Site 690 (Figure 5), because they are not high enough on average to have originated from C_3 land plants (Meyers, 1994; Lamb et al., 2006). The Maud Rise Site 690 core is classified as a nannofossil and foraminifera bearing calcareous ooze throughout our sampling interval (Shipboard Scientific Party, 1988b), which is in agreement with our cross plot of $\delta^{13}C_{org}$ and C/N

(atomic) (Figure 6) in regards to the source of the OM. $\delta^{13}C_{org}$ values range from -33.5 to -25.2 ‰ through our sampled intervals at Maud Rise (Figure 4, Figure 6). Lower $\delta^{13}C_{org}$ values in the -30‰'s are known to occur in phytoplankton of the high latitude Weddell Sea and Southern Ocean, where our core was taken from, as the relatively cooler waters at high latitudes can accommodate increased dissolved CO_2, which allows for greater discrimination against the heavier carbon isotope, ^{13}C, by the phytoplankton (Rau et al., 1989). Some of our lowest $\delta^{13}C_{org}$ values could also reflect significant degradation of their source OM. For example, phytoplankton lipids have lower $\delta^{13}C_{org}$ values in comparison to hemicellulose, cellulose, total sugars and amino acids (Degens et al., 1968). Evidence of oxic conditions across the K-Pg boundary at Maud Rise from our $\delta^{15}N$ values (Figure 5), benthic foraminiferal populations that do not tolerate low oxygen conditions (Alegret and Thomas, 2013), paleoproductivity proxies that indicate reduced OM deposition, and the reddish brown marl depositional environment (Hull and Norris, 2011) support the possibility of OM degradation in an oxic water column. However, without biomarker evidence, this cannot be determined. Still, the majority of our $\delta^{13}C_{org}$ values are still within the range of marine phytoplankton production in the region (Biggs et al., 1988). However, mean $\delta^{13}C_{org}$ values for the late Cretaceous, reddish brown marl interval following the Cretaceous-Paleogene boundary, early Paleocene and late Paleocene are all -27‰ (Figures 4 and 5), suggesting no significant difference in the isotopic composition of the OM deposited on Maud Rise before or after the extinction. This is in contrast to $\delta^{13}C$ values of planktonic foraminifera tests, which have lower $\delta^{13}C$ values in the Paleogene following the extinction event (Stott and Kennett, 1989; Stott and Kennett, 1990; Smit, 1999, Schulte et al., 2010). The shift occurs in the Maud Rise Site

690 cores, and other marine K-Pg boundary sections (Stott and Kennett, 1989; Stott and Kennett, 1990; Smit, 1999, Schulte et al., 2010).

The interpretation of $\delta^{13}C_{org}$ values can provide a nice constraint during the evaluation of $\delta^{15}N$ following the K/Pg boundary, and since a well-known excursion in $\delta^{13}C_{org}$ values and $\delta^{13}C_{carb}$ values associated with the event may occur at this time. The stable isotopes of benthic and planktonic foraminifer across the K-Pg boundary have been investigated at Maud Rise Site 690 (Stott and Kennett, 1989; Stott and Kennett, 1990). They observed a positive shift in $\delta^{13}C_{carb}$ values in both planktonic and benthic foraminifera of the interval directly preceding the K-Pg boundary, which was attributed to warming of the ocean and increased productivity. This was followed by a mild negative excursion in $\delta^{13}C_{carb}$ values of the planktonic foraminifera following the K-Pg boundary of less than 2‰, which they attributed to decreased carbon burial and/or a lack of carbon export to the ocean (Stott and Kennett, 1989; Stott and Kennett, 1990). However, a negative excursion was not observed in the $\delta^{13}C_{carb}$ values of benthic foraminifera (Stott and Kennett, 1989; Stott and Kennett, 1990). Many of the K-Pg boundary sections in the northern hemisphere display two lower $\delta^{13}C_{carb}$ values of shifts of up to 3‰ in planktonic foraminifera, which are separated by a large positive shift (Hollander et al., 1993), so the magnitude of the $\delta^{13}C_{carb}$ shift is reduced at Maud Rise (Stott and Kennett, 1989; Stott and Kennett, 1990). Our $\delta^{13}C_{org}$ values have an almost 0.8‰ positive shift directly before the extinction event, and a negative shift of 1.8‰ through the period of lower $\delta^{15}N$ values occurring through the reddish brown marl interval at Maud Rise (Figure 5).

Additional studies of $\delta^{13}C_{org}$ values across the K-Pg boundary have included multiple depositional settings (Meyers and Simoneit, 1990; Meyers, 1992a; Meyers, 1992b). These studies can compare the changes in the carbon cycle at other locations to the changes at Maud Rise through the K-Pg boundary. Meyers and Simoneit (1990) evaluated a number marine K-Pg boundary locations for their organic carbon isotopic compositions. These locations included Shatsky Rise (ODP Site 577) in the middle latitude Pacific Ocean, the core is also a calcareous nannofossil ooze. Although their data was sparse, Meyers and Simoneit (1990) found the $\delta^{13}C_{org}$ values at Shatsky Rise to be quite variable in comparison to the negative shift observed in $\delta^{13}C_{carb}$ values of planktonic foraminifera across the K-Pg boundary at Shatsky Rise. Meyers and Simoneit (1990) attributed this to the major extinction, and subsequent radiation of new, diverse planktonic species that coincides with the K-Pg boundary. We, however, observe a negative excursion in our $\delta^{13}C_{org}$ values through reddish brown interval following the K-Pg boundary at Maud Rise, and attribute this to a decrease in OM burial and/or export at Maud Rise (Figure 5). Additional locations investigated by Meyers (1992a and 1992b) included a Continental Rise (DSDP Site 605), an outer shelf location at El Kef, Tunisia, and a pelagic carbonate sequence (ODP Site 761 Wombat Plateau). Meyers (1992a) found that the organic carbon isotopes analyzed did not display the same consistent and dramatic negative excursion that observed globally in the inorganic K-Pg stable isotopes. While there was a small shift to lighter $\delta^{13}C_{org}$ values occured at all of these locations across the K-Pg boundary, the shift was not consistent in magnitude like the global record of $\delta^{13}C_{carb}$ values (Meyers, 1992a). They attributed this to the additional influences in the

environment, such as changes in the compositions of the species due to the extinction of planktonic foraminifer associated with the K-Pg boundary (Meyers, 1992a).

$\delta^{13}C_{org}$ values can be used a a proxy to differentiate between marine and terrestrial sources of OM in marine sediments (Schubert and Calvert, 2001). Figure 7 is a cross plot of $\delta^{13}C_{org}$ vs $\delta^{15}N$ values at Maud Rise for the late Cretaceous, K-Pg boundary reddish-brown marl, early Paleocene and late Paleocene. Figure 7 indicates the source of OM did not significantly change during from the late Cretaceous into the late Paleocene. Ten of our 99 $\delta^{13}C_{org}$ values are lower than -28‰. This could be due to heavily degradation of the phytoplankton OM (Degens et al., 1968), or possibly due to contribution of OM from C3 land plants (Meyers, 1994; Lamb et al., 2006). However, we would prefer biomarker data to determine this. The marine phytoplankton at Maud Rise must have been relatively unaffected by changes in the water column oxygen levels towards suboxic conditions, where denitrification predominates, as indicated by shifts to higher $\delta^{15}N$ values in the grey shaded intervals of Figures 4 and 5. Perhaps this is because the phytoplankton were already adapted for highly seasonal climate of the high latitude Southern Ocean. The high latitude planktonic foraminifer phytoplankton in the Antarctic consisted of surviving unspecialized small late Cretaceous species, which eventually migrate to lower latitudes during the early Danian (Keller et al., 1993). Therefore, the oxic water column at Maud Rise may have been an important environmental variable that remained relatively stable through the recovery period (Figure 5). This should be taken into consideration as the marine phytoplankton populations at Maud Rise recovered more rapidly and had less species extinctions than marine phytoplankton from other locations at low and mid latitudes in the northern hemisphere following the extinction event (Stott and Kennett,

1989; Stott and Kennett, 1990; Jiang et al., 2010). In addition, benthic foraminiferal communities at Maud Rise were less affected in comparison to other locations following the K-Pg boundary, and suffered no major extinction throughout our analyzed interval from the late Cretaceous into the late Paleocene (Thomas, 1990; Alegret and Thomas, 2012; Alegret and Thomas, 2013). These additional lines of evidence provide support for our argument of an oxic water column playing an important role during and after the K-Pg extinction event at Maud Rise.

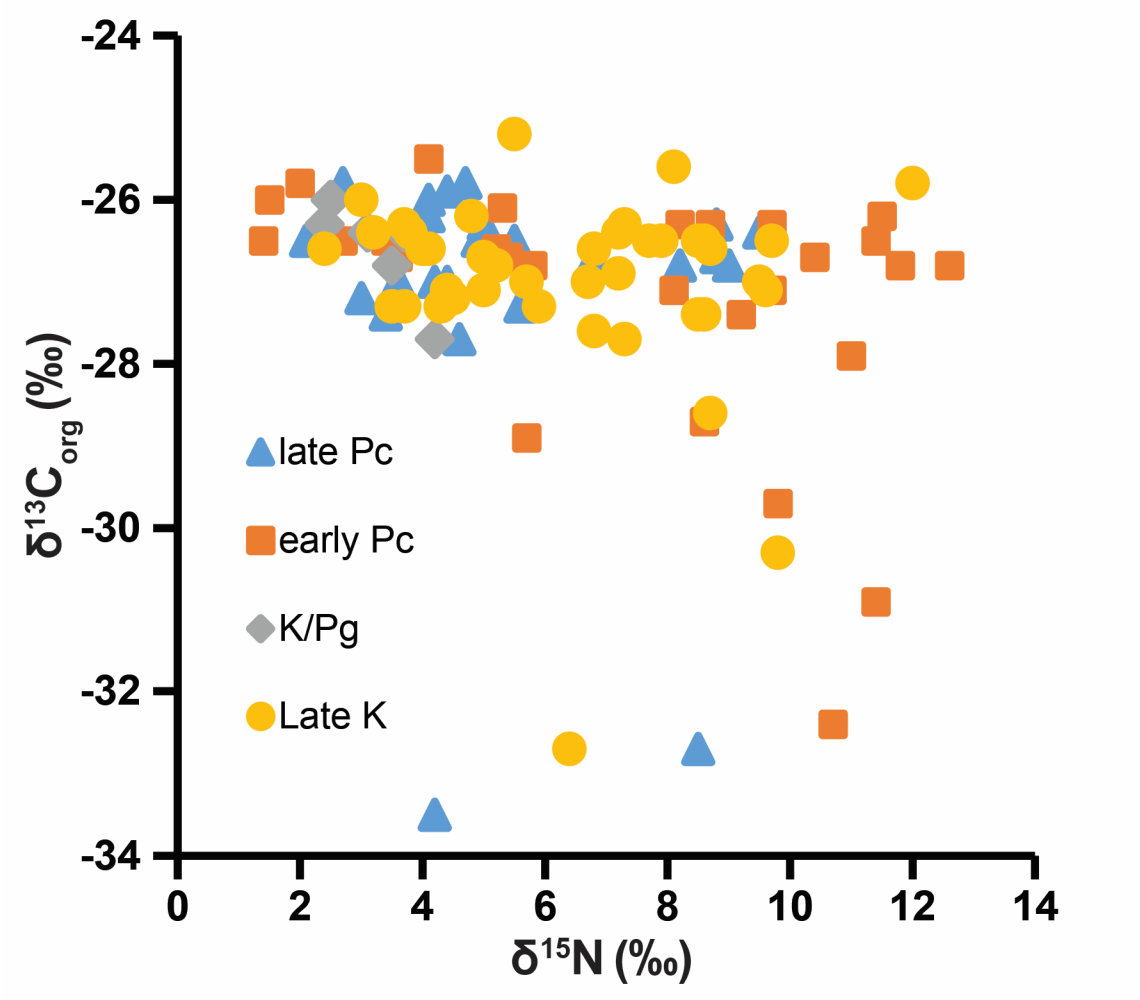

Figure 7. $\delta^{13}C_{org}$ and $\delta^{15}N$ values of decarbonated bulk sediment for the Late Cretaceous (Late K), Cretaceous-Paleogene boundary marl (K/Pg), early Paleocene (early Pc) and late Paleocene (late Pc) at Maud Rise Site 690

Diagenetic Processes at Maud Rise

Previous investigations have concluded that in order to accurately record nitrogen related water column processes in marine sediments, OM must be well preserved (Altabet and Francois, 1994; Altabet et al., 1999). Maud Rise has overall low sedimentation rates, and is located approximately 700 km offshore and 2000 m above the abyssal plane so any terrestrial input is predominately aeolian (Shipboard Scientific Party, 1988b; Thomas et al., 1990). The aeolian dust is derived from the humid Antarctic mainland, with clay content consisting primarily of pedogenic smectite (Kennett and Barker, 1990; Robert and Chamley, 1990; Robert and Maillot, 1990; Ehrmann et al., 1992). Müller and Suess (1979) determined that low sedimentation rates in marine sediments are the most critical factor preventing preservation of organic material in marine sediments. Low sedimentation rates prevent rapid burial of OM, and promote degradation of organic material through increased exposure to oxygen in both the water column and near surface sediment layer (Müller and Suess, 1979). Previously measured TOC concentrations through our analyzed interval at Maud Rise are sparse; however, all are below 0.2% (Thompson and Dow, 1990). We do not know the level of preservation of the OM we analyzed during our investigation. Others disagree that increased oxygen exposure in the water column leads to lower OM preservation, as their findings indicate that OM is equally preserved in both an anoxic basin and the open ocean (Thunnell et al., 2000). Additionally, there is debate as to whether an oxygenated water column or low sedimentation rates are the dominant factor controlling the preservation of OM (Hartnett et al., 1998). Maud Rise has both of these criteria based on our data and the findings of Thomas et al. (1990).

Others have shown evidence of decreases, increases or no change in $\delta^{15}N$ values on geological timescales in well oxygenated, slowly accumulating sediments after deposition, therefore, alteration of the $\delta^{15}N$ values preserved in marine sediments are a matter of some controversy (Kienast, 2000; Robinson et al., 2012; Tesdal et al., 2013). For example, Robinson et al. (2012) presents data compilation figures showing a trend of increasing $\delta^{15}N$ values with decreasing sedimentation rates. Our Maud Rise data is not in agreement with this trend through the K-Pg boundary. Calculated sedimentation rates in the reddish brown marl following the boundary (≈1 m/m.y.) are the lowest of the entire study interval (Hull and Norris, 2011), and our data have 6 consistently lower $\delta^{15}N$ values in the reddish brown marl (Figure 5). The processes behind diagenetic affects to $\delta^{15}N$ values in our depositional environment are not yet well understood, as a wide variety of pelagic ocean sedimentary $\delta^{15}N$ records on geological timescales does not yet exist. Oxic incubation experiments over 120 days have found that $\delta^{15}N$ values initially increase before returning to a value indistinguishable from the original $\delta^{15}N$ values (Lehmann et al., 2002). Therefore, our sedimentary $\delta^{15}N$ values are likely to be their original value in the surface ocean if this process also occurs on geological timescales.

CHAPTER V

CONCLUSION

Oxic conditions occurred through the reddish brown marl interval of the K-Pg boundary at Maud Rise, and Maud Rise was oxic to suboxic during the late Cretaceous, early and late Paleocene intervals analyzed in this study. We determined this through sedimentary $\delta^{15}N$ values, which have a previously established relationship to water column oxygen levels (Altabet and Francois, 1994; Ganeshram et al., 2002; Quan et al., 2008; Sigman et al, 2009; Ryabenko et al., 2012; Quan et al., 2013). Oxic conditions attributed to the more rapid recovery of calcareous plankton at Maud Rise in comparison to mid and low latitude locations (Stott and Kennett, 1989; Stott and Kennett, 1990, Jiang et al., 2010). The oxic water column is consistent with lack of extinction in benthic foraminifera (Thomas, 1990; Alegret and Thomas, 2012; Alegret and Thomas, 2013), because surviving/existing taxa were already adapted to the prevailing oxic water column conditions, an important environmental variable. Southern, high latitude locations (i.e., Maud Rise) had greater species survival rates and lower diversity in comparison to

low and mid latitude locations, as well as the northern hemisphere in general, where the Chicxulub impact occurred (Jiang et al., 2010) and a shift to lower oxygen levels was observed (Kaiho et al., 1999). The sedimentary organic matter analyzed in this study originated primarily from marine phytoplankton, with occasional input from C3 plants (Meyers, 1994; Lamb et al., 2006). Our low $\delta^{13}C_{org}$ values are typical of marine phytoplankton formed in the cooler water temperatures of the high latitude Weddell Sea of Antarctica (Biggs et al., 1988; Rau et al., 1989**)**. The relatively cooler waters (in comparison to low and mid latitude) allow for greater concentrations of dissolved CO_2 in the water column, which, together with low production, allowed for increased selectivity by the phytoplankton (Rau et al., 1989**)**. $\delta^{13}C_{org}$ values trend lower overall through the reddish-brown marl K-Pg boundary interval at Maud Rise in relation to the late Cretaceous $\delta^{13}C_{org}$ value that is nearest to the K-Pg boundary. These lower $\delta^{13}C_{org}$ values reflect a period of depressed marine production or decreased export of OM to the sediments due to a disruption the ocean's biological carbon pump (D'Hondt, 2005; Schulte et al., 2010).

We conclude that consistent water column oxygenation levels provided the mechanism for rapid resurgence of the surviving calcareous plankton at Maud Rise in comparison to low and mid latitude locations, since species were already adapted to the high oxygen concentrations, an important variable in the marine environment.

Further Research

Additional methods could further resolve sedimentation rates to better interpolate geological time between events at Maud Rise, and yield evidence of previously unknown

relationships to changes the nitrogen cycle. Therefore, we recommend astronomical tuning of the Maud Rise Site 690 archive cores using the methods similar to those in Westerhold et al. (2008) and Hilgen et al. (2010), this would allow us to better evaluate changes in our $\delta^{15}N$ values.

Biomarkers provide a molecular fossil record and can be a useful tool in evaluating depositional environments. For our purposes, the evaluation of biomarkers through the K-Pg boundary at Maud Rise Site 690 might reveal more information about the source or sources of OM deposited at the time.

Using Inductively Coupled Plasma Mass Spectrometry (ICP-MS) to determine concentrations of redox sensitive trace metals at Maud Rise Site 690 would provide additional information about redox conditions (Tribovillard et al., 2006). However, anyone considering trace metals as an indicator of redox conditions following the K-Pg boundary should consider the additional input of trace metals into the water column from the Chicxulub impact (Kaiho et al., 1999; Jiang et al., 2010) during interpretation of these data.

During the course of this investigation we learned that ODP Sites 692 and 693 contained Early and Late Cretaceous sediments consisting of non-laminated black shales with very high TOC content; these sites are located on the shelf of Antarctica in the eastern Weddell Sea (Shipboard Scientific Party, 1988c; Thompson and Dow, 1990). An investigation of changes in $\delta^{15}N$ values related to the disappearance of the black shales through this interval could reveal whether the ventilation of the basin was abrupt, or a

series of pulses, and thus relate changes in the marine nitrogen cycle to a poorly understood tectonic event.

REFERENCES

Adams, J. B., Mann, M. E., & D'Hondt, S. (2004). The Cretaceous-Tertiary extinction: Modeling carbon flux and ecological response. *Paleoceanography*, **19**, 1-13.

Alegret, L., & Thomas, E. (2009). Food supply to the seafloor in the Pacific Ocean after the Cretaceous-Paleogene boundary event. *Marine Micropaleontology*, **73**, 105-116.

Alegret, L., Thomas, E., & Lohmann, K. C. (2012). End-Cretaceous marine mass extinction not caused by productivity collapse. *Proceedings of the National Academy of Sciences*, **109**, 728-732.

Alegret, L., & Thomas, E. (2013). Benthic foraminifer across the Cretaceous-Paleogene boundary in the Southern Ocean (ODP Site 690): Diversity, food and carbonate saturation. *Marine Micropaleontology*, **105**, 40-51.

Altabet, M. A., & Francois, R. (1994). Sedimentary nitrogen isotopic ratio as a recorder for surface ocean nitrate utilization. *Global Biogeochemical Cycles*, **8**, 103-116.

Altabet, M. A., Murray, D. W., & Prell, W. L. (1999). Climatically linked oscillations in Arabian Sea denitrification over the past 1 my: Implications for the marine N cycle. *Paleoceanography*, **14**, 732-743.

Altabet, M. A. (2006). Isotopic Tracers of the Marine Nitrogen Cycle: Present and Past. In J. K. Volkman (Ed.), *Marine Organic Matter: Biomarkers, Isotopes and DNA,* **2N**, 251-293. Springer Berlin Heidelberg.

Alvarez, L. W., Alvarez, W., Asaro, F., & Michel, H. V. (1980). Extraterrestrial cause for the Cretaceous-Tertiary extinction. *Science*, **208**, 1095-1108.

Arthur, M. A., Zachos, J. C., & Jones, D. S. (1987). Primary productivity and the Cretaceous/Tertiary boundary event in the oceans. *Cretaceous Research*, **8**, 43-54.

Barker, P. F., Leg 113 Shipboard Scientific Party (1987). Glacial History of Antarctica. *Nature*, **328**, 115-116.

Barrera, E., & Keller, G. (1994). Productivity across the Cretaceous/Tertiary boundary in high latitudes. *Geological Society of America Bulletin*, **106**, 1254-1266.

Blakey, R. (2011). *Global Paleogeography*, http://cpgeosystems.com

Bernaola, G., & Monechi, S. (2007). Calcareous nannofossil extinction and survivorship across the Cretaceous− Paleogene boundary at Walvis Ridge (ODP Hole 1262C, South Atlantic Ocean). *Palaeogeography, Palaeoclimatology, Palaeoecology*, **255**, 132-156.

Biggs, D.C., Berkowitz, S.P., Altabet, M.A., Bidigare, R.R., DeMaster, D.J., Dunbar, R.B., Leventer, A., Macko, S.A., Nittrouer, C.A., and Ondrusek, M.E., 1988. A cooperative study of upper-ocean particulate fluxes in the Weddell Sea. *In* Barker, P.E, Kennett, J.P., et al., *Proceedings of the Ocean Drilling Program, Initial Reports*, **113**, College Station, TX, 77–86.

Boersma, A., & Shackleton, N. J. (1981). Oxygen-and carbon-isotope variations and planktonic-foraminifer depth habitats, Late Cretaceous to Paleocene, central Pacific, Deep Sea Drilling Project Sites 463 and 465. *Initial Reports of the Deep Sea Drilling Project*, **62**, 513-526.

Bown, P. (2005). Selective calcareous nannoplankton survivorship at the Cretaceous-Tertiary boundary. *Geology*, **33**, 653-656.

Brisman, K., Engel, M. H., & Macko, S. A. (2001). Distribution, stereochemistry, and stable isotope composition of amino acids in K/T boundary sediments. *Precambrian Research*, **106**, 59-77.

Brunner, B., Contreras, S., Lehmann, M. F., Matantseva, O., Rollog, M., Kalvelage, T., Klockgether, G., Lavik, G., Jetten, M. S. M., Kartal, B., & Kuypers, M. M. M. (2013). Nitrogen isotope effects induced by anammox bacteria. *Proceedings of the National Academy of Sciences*, **110**, 18994-18999.

Capone, D. G., Zehr, J. P., Paerl, H. W., Bergman, B., & Carpenter, E. J. (1997). Trichodesmium, a globally significant marine cyanobacterium. *Science*, **276**, 1221-1229.

Capone, D. G., Bronk, D. A., Mulholland, M. R., & Carpenter, E. J. (Eds.). (2008). *Nitrogen in the Marine Environment*. Academic Press.

Casciotti, K. L., & Buchwald, C. (2012). Insights on the marine microbial nitrogen cycle from isotopic approaches to nitrification. *Frontiers in Microbiology*, **3**. 133.

Cline, J. D., & Kaplan, I. R. (1975). Isotopic fractionation of dissolved nitrate during denitrification in the eastern tropical North Pacific Ocean. *Marine Chemistry*, **3**, 271-299.

Codispoti, L. A., Brandes, J. A., Christensen, J. P., Devol, A. H., Naqvi, S. W. A., Paerl, H. W., & Yoshinari, T. (2001). The oceanic fixed nitrogen and nitrous oxide budgets: Moving targets as we enter the anthropocene? *Scientia Marina,* **65**, 85–105

Corfield, R. M. (1994). Palaeocene oceans and climate: An isotopic perspective. *Earth-Science Reviews*, **37**, 225-252.

Degens, E. T., Behrendt, M., Gotthardt, B., & Reppmann, E. (1968). Metabolic fractionation of carbon isotopes in marine plankton –II. Data on samples collected off the coasts of Peru and Ecuador. *Deep-Sea Research,* **15,** 11-20.

D'Hondt, S., Donaghay, P., Zachos, J. C., Luttenberg, D., & Lindinger, M. (1998). Organic carbon fluxes and ecological recovery from the Cretaceous-Tertiary mass extinction. *Science*, **282**, 276-279.

D'Hondt, S. (2005). Consequences of the cretaceous/paleogene mass extinction for marine ecosystems. *Annual Review of Ecology Evolution and Systematics,* **36**, 295-317.

Dymond, J. (1981). Geochemistry of Nazca Plate Surface Sediments - an Evaluation of Hydrothermal, Biogenic, Detrital, and Hydrogenous Sources. *Geological Society of America Memoirs,* **154**, 133-173.

Dymond, J., Suess, E., & Lyle, M. (1992). Barium in deep-sea sediment: A geochemical proxy for paleoproductivity. *Paleoceanography*, **7**, 163-181.

Ehrmann, W. U., Melles, M., Kuhn, G., & Grobe, H. (1992). Significance of clay mineral assemblages in the Antarctic Ocean. *Marine Geology*, **107**, 249-273.

Esmeray-Senlet, S., Wright, J. D., Olsson, R. K., Miller, K. G., Browning, J. V., & Quan, T. M. (2015). Evidence for reduced export productivity following the Cretaceous-Paleogene mass extinction. *Paleoceanography*, **30**, 718-738.

Francois, R., Honjo, S., Manganini, S. J., & Ravizza, G. E. (1995). Biogenic barium fluxes to the deep sea: Implications for paleoproductivity reconstruction. *Global Biogeochemical Cycles*, **9**, 289-303.

Ganeshram, R. S., Pedersen, T. F., Calvert, S., & François, R. (2002). Reduced nitrogen fixation in the glacial ocean inferred from changes in marine nitrogen and phosphorus inventories. *Nature*, **415**, 156-159.

Gruber, N., & Galloway, J. N. (2008). An Earth-system perspective of the global nitrogen cycle. *Nature,* **451**, 293-296.

Haq, B. U., Hardenbol, J., & Vail, P. R. (1987). Chronology of fluctuating sea levels since the Triassic. *Science*, **235**, 1156-1167.

Haq, B. U. (2014). Cretaceous eustasy revisited. *Global and Planetary Change*, **113**, 44-58.

Hartnett, H. E., Keil, R. G., Hedges, J. I., & Devol, A. H. (1998). Influence of oxygen exposure time on organic carbon preservation in continental margin sediments. *Nature*, **391**, 572-575.

Hilgen, F. J., Kuiper, K. F., & Lourens, L. J. (2010). Evaluation of the astronomical time scale for the Paleocene and earliest Eocene. *Earth and Planetary Science Letters*, **300**, 139-151.

Hollander, D. J., McKenzie, J. A., & Hsü, K. J. (1993). Carbon isotope evidence for unusual plankton blooms and fluctuations of surface water CO_2 in "Strangelove Ocean" after terminal Cretaceous event. *Palaeogeography, Palaeoclimatology, Palaeoecology*, **104**, 229-237.

Hsü, K. J., He, Q., Mckenzie, J. A., Weissert, H., Perchnielsen, K., Oberhansli, H., Kelts, K., Labrecque, J., Tauxe, L., Krahenbuhl, U., Percival, S. F., Wright, R., Karpoff, A. M., Petersen, N., Tucker, P., Poore, R. Z., Gombos, A. M., Pisciotto, K., Carman, M. F., & Schreiber, E. (1982). Mass mortality and its environmental and evolutionary consequences. *Science*, **216**, 249-256.

Hsü, K. J., & McKenzie, J. A. (1985). A "Strangelove" ocean in the earliest Tertiary. *Geophysical Monograph Series*, **32**, 487-492.

Hull, P. M., & Norris, R. D. (2011). Diverse patterns of ocean export productivity change across the Cretaceous-Paleogene boundary: New insights from biogenic barium. *Paleoceanography*, **26**, 1-10.

Hull, P. M., Franks, P. J., & Norris, R. D. (2011a). Mechanisms and models of iridium anomaly shape across the Cretaceous–Paleogene boundary. *Earth and Planetary Science Letters*, **301**, 98-106.

Hull, P. M., Norris, R. D., Bralower, T. J., & Schueth, J. D. (2011b). A role for chance in marine recovery from the end-Cretaceous extinction. *Nature Geoscience*, **4**, 856-860.

Kaiho, K., Kajiwara, Y., Tazaki, K., Ueshima, M., Takeda, N., Kawahata, H., Arinobu, T., Ishiwatari, R., Hirai, A., & Lamolda, M. A. (1999). Oceanic primary productivity and dissolved oxygen levels at the Cretaceous/Tertiary boundary: Their decrease, subsequent warming, and recovery. *Paleoceanography,* **14**, 511-524.

Kaiho, K., Oshima, N., Adachi, K., Adachi, Y., Mizukami, T., Fujibayashi, M., & Saito, R. (2016). Global climate change driven by soot at the K-Pg boundary as the cause of the mass extinction. *Scientific Reports*, **6**, 28427.

Kajiwara, Y., & Kaiho, K. (1992). Oceanic anoxia at the Cretaceous/Tertiary boundary supported by the sulfur isotopic record. *Palaeogeography, Palaeoclimatology, Palaeoecology*, **99**, 151-162.

Keller, G., Barrera, E., Schmitz, B., & Mattson, E. (1993). Gradual mass extinction, species survivorship, and long-term environmental changes across the Cretaceous-Tertiary boundary in high latitudes. *Geological Society of America Bulletin*, **105**, 979-997.

Keller, G. (2003). Biotic effects of impacts and volcanism. *Earth and Planetary Science Letters*, **215**, 249-264.

Keller, G., Adatte, T., Stinnesbeck, W., Stüben, D., Berner, Z., Kramar, U., & Harting, M. (2004). More evidence that the Chicxulub impact predates the K/T mass extinction. *Meteoritics & Planetary Science*, **39**, 1127-1144.

Kennedy, P., Kennedy, H., & Papadimitriou, S. (2005). The effect of acidification on the determination of organic carbon, total nitrogen and their stable isotopic composition in algae and marine sediment. *Rapid Communications in Mass Spectrometry*, **19**, 1063-1068.

Kennett, J. P., & Barker, P. F. (1990). Latest Cretaceous to Cenozoic climate and oceanographic developments in the Weddell Sea, Antarctica: an ocean-drilling perspective. *In* Barker, P.F., Kennett, J.P., et al., *Proceedings of the Ocean Drilling Program, Scientific Results*, **113**, College Station, TX, 937-960.

Kienast, M. (2000). Unchanged nitrogen isotopic composition of organic matter in the South China Sea during the last climatic cycle: Global implications. *Paleoceanography*, **15**, 244-253.

Kump, L. R. (1991). Interpreting carbon-isotope excursions: Strangelove oceans. *Geology*, **19**, 299-302.

Kuypers, M. M. M., Sliekers, A. O., Lavik, G., Schmid, M., Jorgensen, B. B., Kuenen, J. G., Damste, J. S. S., Strous, M., & Jetten, M. S. M. (2003). Anaerobic ammonium oxidation by anammox bacteria in the Black Sea. *Nature*, **422**, 608-611.

Jiang, S., Bralower, T. J., Patzkowsky, M. E., Kump, L. R., & Schueth, J. D. (2010). Geographic controls on nannoplankton extinction across the Cretaceous/Palaeogene boundary. *Nature Geoscience*, **3**, 280-285.

Lamb, A. L., Wilson, G. P., & Leng, M. J. (2006). A review of coastal palaeoclimate and relative sea-level reconstructions using $\delta^{13}C$ and C/N ratios in organic material. *Earth-Science Reviews*, **75**, 29-57.

Lehmann, M. F., Bernasconi, S. M., Barbieri, A., & McKenzie, J. A. (2002). Preservation of organic matter and alteration of its carbon and nitrogen isotope composition during simulated and in situ early sedimentary diagenesis. *Geochimica Et Cosmochimica Acta,* **66**, 3573-3584.

Macko, S. A., Fogel, M. L., Hare, P. E., & Hoering, T. C. (1987). Isotopic fractionation of nitrogen and carbon in the synthesis of amino acids by microorganisms. *Chemical Geology: Isotope Geoscience Section*, **65**, 79-92.

MacLeod, K. G., Whitney, D. L., Huber, B. T., & Koeberl, C. (2007). Impact and extinction in remarkably complete Cretaceous-Tertiary boundary sections from Demerara Rise, tropical western North Atlantic. *Geological Society of America Bulletin*, **119**, 101-115.

Meyers, P. A., & Simoneit, B. R. (1990). Global comparisons of organic matter in sediments across the Cretaceous/Tertiary boundary. *Organic Geochemistry*, **16**, 641-648.

Meyers, P. A. (1992a). Changes in organic carbon stable isotope ratios across the K/T boundary: global or local control?. *Chemical Geology: Isotope Geoscience Section*, **101**, 283-291.

Meyers, P. A. (1992b). Data report: The Cretaceous/Tertiary boundary at sites 761 and 762 (northwest Australian margin), at El Kef (Tunisia), and in the Negev Desert (Israel): A comparison of the organic geochemical records. *In* von Rad, U., Haq, B.U., et al., *Proceedings of the Ocean Drilling Program, Scientific Results,* **122**, 881-885.

Meyers, P. A. (1994). Preservation of elemental and isotopic source identification of sedimentary organic matter. *Chemical Geology*, **114**, 289-302.

Michel, H. V., Asaro, F., Alvarez, W., & Alvarez, L. W. (1990). Geochemical studies of the Cretaceous-Tertiary Boundary in ODP Holes 689B and 690C. *In* Barker, P.F., Kennett, J.P., et al., *Proceedings of the Ocean Drilling Program, Scientific Results*, **113**, College Station, TX, 159-168.

Minagawa, M., & Wada, E. (1984). Stepwise enrichment of ^{15}N along food chains: further evidence and the relation between $\delta^{15}N$ and animal age. *Geochimica Et Cosmochimica Acta*, **48**, 1135-1140.

Minagawa, M., & Wada, E. (1986). Nitrogen Isotope Ratios of Red Tide Organisms in the East-China-Sea - a Characterization of Biological Nitrogen Fixation. *Marine Chemistry,* **19**, 245-259.

Miyake, Y., & Wada, E. (1971). The isotope effect on the nitrogen in biochemical, oxidation-reduction reactions. *Recorded Oceanography Works of Japan*, **11**, 1-6.

Müller, P. J., & Suess, E. (1979). Productivity, sedimentation rate, and sedimentary organic matter in the oceans—I. Organic carbon preservation. *Deep Sea Research Part A. Oceanographic Research Papers*, **26**, 1347-1362.

O'Connell, S.B., (1990). Sedimentary facies and depositional environment of the Lower Cretaceous east Antarctic margin: Sites 692 and 693. *In* Barker, P.F., Kennett, J.P., et al., *Proceedings of the Ocean Drilling Program, Scientific Results*, **113**, College Station, TX, 71-88.

Olsson, R. K., & Liu, C. (1993). Controversies on the placement of Cretaceous-Paleogene boundary and the K/P mass extinction of planktonic foraminifera. *Palaios*, 127-139.

Pospichal, J. J., & Wise Jr, S. W. (1990). Calcareous nannofossils across the K/T boundary, ODP hole 690C, Maud Rise, Weddell Sea. *In* Barker, P.F., Kennett, J.P., et al., *Proceedings of the Ocean Drilling Program, Scientific Results*, **113**, College Station, TX, 515-532.

Quan, T. M., van de Schootbrugge, B., Field, M. P., Rosenthal, Y., & Falkowski, P. G. (2008). Nitrogen isotope and trace metal analyses from the Mingolsheim core (Germany): Evidence for redox variations across the Triassic-Jurassic boundary. *Global Biogeochemical Cycles,* **22.** 1-14.

Quan, T.M., & Falkowski, P.G. (2009). Redox control of N:P ratios in aquatic ecosystems. *Geobiology*, **7**, 124–139

Quan, T.M., Wright, J.D., Falkowski, P.G., (2013). Co-variation of nitrogen isotopes and redox states through glacial-interglacial cycles in the Black Sea. *Geochimica et Cosmochimica Acta,* **112**, 305–320.

Rau, G. H., Takahashi, T., & Des Marais, D. J. (1989). Latitudinal variations in plankton C: implications for CO and productivity in past oceans. *Nature*, **341**, 165.

Ravizza, G., & VonderHaar, D. (2012). A geochemical clock in earliest Paleogene pelagic carbonates based on the impact-induced Os isotope excursion at the Cretaceous-Paleogene boundary. *Paleoceanography*, **27**, 1-15.

Renne, P. R., Sprain, C. J., Richards, M. A., Self, S., Vanderkluysen, L., & Pande, K. (2015). State shift in Deccan volcanism at the Cretaceous-Paleogene boundary, possibly induced by impact. *Science*, **350**, 76-78.

Robert, C., & Chamley, H. (1990). Paleoenvironmental significance of clay mineral associations at the Cretaceous-Tertiary passage. *Palaeogeography, Palaeoclimatology, Palaeoecology*, **79**, 205-219.

Robert, C., & Maillot, H. (1990). Paleoenvironments in the Weddell Sea area and Antarctic climates, as deduced from clay mineral associations and geochemical data, ODP Leg 113. *In* Barker, P.F., Kennett, J.P., et al., *Proceedings of the Ocean Drilling Program, Scientific Results*, **113**, College Station, TX, 51-70.

Robinson, N., Ravizza, G., Coccioni, R., Peucker-Ehrenbrink, B., & Norris, R. (2009). A high-resolution marine $^{187}Os/^{188}Os$ record for the late Maastrichtian: Distinguishing the chemical fingerprints of Deccan volcanism and the KP impact event. *Earth and Planetary Science Letters*, **281**, 159-168.

Robinson, R. S., Kienast, M., Albuquerque, A. L., Altabet, M., Contreras, S., Holz, R. D., Dubois, N., Francois, R., Galbraith, E., Hsu, T. C., Ivanochko, T., Jaccard, S., Kao, S. J., Kiefer, T., Kienast, S., Lehmann, M. F., Martinez, P., McCarthy, M., Mobius, J., Pedersen, T., Quan, T. M., Ryabenko, E., Schmittner, A., Schneider, R., Schneider-Mor, A., Shigemitsu, M., Sinclair, D., Somes, C., Studer, A., Thunell, R., & Yang, J. Y. (2012). A review of nitrogen isotopic alteration in marine sediments. *Paleoceanography,* **27**. 1-13.

Ryabenko, E., Kock, A., Bange, H. W., Altabet, M. A., & Wallace, D. W. (2012). Contrasting biogeochemistry of nitrogen in the Atlantic and Pacific Oxygen Minimum Zones. *Biogeosciences*, **9**, 203-215.

Schoene, B., Samperton, K. M., Eddy, M. P., Keller, G., Adatte, T., Bowring, S. A., Gertsch, B. (2015). U-Pb geochronology of the Deccan Traps and relation to the end-Cretaceous mass extinction. *Science*, **347**, 182-184.

Schubert, C. J., & Calvert, S. E. (2001). Nitrogen and carbon isotopic composition of marine and terrestrial organic matter in Arctic Ocean sediments: implications for nutrient utilization and organic matter composition. *Deep Sea Research Part I: Oceanographic Research Papers*, **48**, 789-810.

Sepúlveda, J., Wendler, J. E., Summons, R. E., & Hinrichs, K. U. (2009). Rapid resurgence of marine productivity after the Cretaceous-Paleogene mass extinction. *Science*, **326**, 129-132.

Shemesh, A., Macko, S. A., Charles, C. D., & Rau, G. H. (1993). Isotopic evidence for reduced productivity in the glacial Southern Ocean. *Science*, **262**, 407-410.

Shipboard Scientific Party, 1988a. Introduction and objectives. *In* Barker, P.F., Kennett, J.P., et al., *Proceedings of the Ocean Drilling Program, Initial Reports*, **113**, College Station, TX, 5-11.

Shipboard Scientific Party, 1988b. Site 690. *In* Barker, P.F., Kennett, J.P., et al., *Proceedings of the Ocean Drilling Program, Initial Reports*, **113**, College Station, TX, 183-292.

Shipboard Scientific Party, 1988c. Site 693. *In* Barker, P.F., Kennett, J.P., et al., *Proceedings of the Ocean Drilling Program, Initial Reports*, **113**, College Station, TX, 329-447.

Schulte, P., Alegret, L., Arenillas, I., Arz, J. A., Barton, P. J., Bown, P. R., Bralower, T. J., Christeson, G. L., Claeys, P., Cockell, C. S., Collins, G. S., Deutsch, A., Goldin, T. J., Goto, K., Grajales-Nishimura, J. M., Grieve, R. A. F., Gulick, S. P. S., Johnson, K. R., Kiessling, W., Koeberl, C., Kring, D. A., MacLeod, K. G., Matsui, T., Melosh, J., Montanari, A., Morgan, J. V., Neal, C. R., Nichols, D. J., Norris, R. D., Pierazzo, E., Ravizza, G., Rebolledo-Vieyra, M., Reimold, W. U., Robin, E., Salge, T., Speijer, R. P., Sweet, A. R., Urrutia-Fucugauchi, J., Vajda, V., Whalen, M. T., & Willumsen, P. S. (2010). The Chicxulub Asteroid Impact and Mass Extinction at the Cretaceous-Paleogene Boundary. *Science,* **327**, 1214-1218.

Sibert, E. C., Hull, P. M., & Norris, R. D. (2014). Resilience of Pacific pelagic fish across the Cretaceous/Palaeogene mass extinction. *Nature Geoscience*, **7**, 667-670.

Sigman, D. M., DiFiore, P. J., Hain, M. P., Deutsch, C., & Karl, D. M. (2009). Sinking organic matter spreads the nitrogen isotope signal of pelagic denitrification in the North Pacific. *Geophysical Research Letters*, **36**, 1-5.

Smit, J. (1999). The global stratigraphy of the Cretaceous-Tertiary boundary impact ejecta. *Annual Review of Earth and Planetary Sciences*, **27**, 75-113.

Stott, L. D., & Kennett, J. P. (1989). New constraints on early Tertiary palaeoproductivity from carbon isotopes in foraminifera. *Nature*, **342**, 526-529.

Stott, L. D., & Kennett, J. P. (1990). The paleoceanographic and paleoclimatic signature of the Cretaceous-Paleogene boundary in the Antarctic: stable isotopic results from

ODP Leg 113. *In* Barker, P.F., Kennett, J.P., et al., *Proceedings of the Ocean Drilling Program, Scientific Results*, **113**, College Station, TX, 829-848.

Tesdal, J. E., Galbraith, E. D., & Kienast, M. (2013). Nitrogen isotopes in bulk marine sediment: linking seafloor observations with subseafloor records. *Biogeosciences*, **10**, 101-118.

Thomas, E., (1990). Late Cretaceous through Neogene deep-sea benthic foraminifers (Maud Rise, Weddell Sea, Antarctica). *In* Barker, P.F., Kennett, J.P., et al., *Proceedings of the Ocean Drilling Program, Scientific Results*, **113**, College Station, TX, 571-594.

Thomas, E., Barrera, E., Hamilton, N., Huber, B.T., Kennett, J.P., O'Connell, S.B., Pospichal, J.J., Speiß, V., Stott, L.D., Wei, W., and Wise, S.W., Jr. (1990). Upper Cretaceous–Paleogene stratigraphy of Sites 689 and 690, Maud Rise (Antarctica). *In* Barker, P.F., Kennett, J.P., et al., *Proceedings of the Ocean Drilling Program, Scientific Results*, **113**, College Station, TX, 901-914.

Thompson, K.F.M., and Dow, W.G. (1990). Investigation of Cretaceous and Tertiary kerogens in sediments of the Weddell Sea. *In* Barker, P.F., Kennett, J.P., et al., *Proceedings of the Ocean Drilling Program, Scientific Results*, **113**, College Station, TX, 189-197.

Thunell, R. C., Varela, R., Llano, M., Collister, J., Karger, F. M., & Bohrer, R. (2000). Organic carbon fluxes, degradation, and accumulation in an anoxic basin: sediment trap results from the Cariaco Basin. *Limnology and Oceanography*, **45**, 300-308.

Tribovillard, N., Algeo, T. J., Lyons, T., & Riboulleau, A. (2006). Trace metals as paleoredox and paleoproductivity proxies: an update. *Chemical Geology*, **232**, 12-32.

Turner, J. T. (2002). Zooplankton fecal pellets, marine snow and sinking phytoplankton blooms. *Aquatic Microbial Ecology*, **27**, 57-102.

Wada, E. (1980). Nitrogen isotope fractionation and its significance in biogeochemical processes occurring in marine environments. *Isotope Marine Chemistry*, **1**, 375-398.

Wada, E., Terazaki, M., Kabaya, Y., & Nemoto, T. (1987). ^{15}N and ^{13}C abundances in the Antarctic Ocean with emphasis on the biogeochemical structure of the food web. *Deep-Sea Research*, **34**, 829-841.

Westerhold, T., Rohl, U., Raffi, I., Fornaciari, E., Monechi, S., Reale, V., Bowles, J., & Evans, H. F. (2008). Astronomical calibration of the Paleocene time. *Palaeogeography Palaeoclimatology Palaeoecology,* **257**, 377-403.

Zachos, J. C., & Arthur, M. A. (1986). Paleoceanography of the Cretaceous/Tertiary boundary event: inferences from stable isotopic and other data. *Paleoceanography*, **1**, 5-26.

Zachos, J. C., Arthur, M. A. and Dean, W. E. (1989), Geochemical evidence for suppression of pelagic marine productivity at the Cretaceous/Tertiary boundary, *Nature*, **337**, 61-64.

APPENDICES

Appendix A

Correlation between Ocean Drilling Program sample information and abbreviations used during EA/IRMS analyses (*note*-samples were randomized for analyses, data below presented with respect to increasing sample depth)

Sample Vial #	Leg	Site	Hole	Core	Type	Section	Top(cm)	Bot(cm)	Depth(mbsf)
65	113	690	B	23	H	1	80.5	86.0	192.01
16	113	690	B	23	H	2	78.0	79.0	193.48
19	113	690	B	23	H	3	81.0	82.0	195.01
87	113	690	B	23	H	4	82.5	83.5	196.53
106	113	690	B	23	H	5	53.0	54.0	197.73
62	113	690	B	24	H	1	80.0	81.0	199.00
68	113	690	B	24	H	2	81.0	82.0	200.51
95	113	690	B	24	H	3	81.0	82.0	202.01
44	113	690	B	24	H	4	81.5	82.5	203.52
73	113	690	B	25	H	1	138.0	139.0	205.58
80	113	690	B	25	H	2	82.0	83.0	206.52
17	113	690	B	25	H	3	78.5	79.5	207.99
22	113	690	B	25	H	4	79.0	80.0	209.49
10	113	690	B	25	H	5	57.5	58.5	210.78
111	113	690	B	25	H	6	97.0	98.0	212.67
28	113	690	C	12	X	2	42.5	43.5	215.83
100	113	690	C	13	X	1	48.5	49.5	224.09
118	113	690	C	13	X	1	104.0	105.0	224.64
29	113	690	C	13	X	2	63.0	64.0	225.73
117	113	690	C	13	X	2	121.0	122.0	226.31
66	113	690	C	13	X	3	56.0	57.0	227.16
2	113	690	C	13	X	3	124.0	125.0	227.84
34	113	690	C	13	X	4	57.0	58.0	228.67
77	113	690	C	13	X	4	140.0	141.0	229.50
47	113	690	C	13	X	5	46.0	47.0	230.06
58	113	690	C	13	X	5	124.5	125.5	230.85
51	113	690	C	13	X	6	15.0	16.0	231.25
98	113	690	C	13	X	6	96.0	97.0	232.06
107	113	690	C	14	X	1	25.0	26.0	233.45
123	113	690	C	14	X	1	72.0	73.0	233.92
37	113	690	C	14	X	1	136.0	137.0	234.56
93	113	690	C	14	X	2	11.0	12.0	234.81
122	113	690	C	14	X	2	85.0	86.0	235.55
8	113	690	C	14	X	2	139.0	140.0	236.09

Sample Vial #	Leg	Site	Hole	Core	Type	Section	Top(cm)	Bot(cm)	Depth(mbsf)
11	113	690	C	14	X	3	20.0	21.0	236.40
79	113	690	C	14	X	3	81.0	82.0	237.01
86	113	690	C	14	X	3	140.0	141.0	237.60
88	113	690	C	14	X	4	16.0	17.0	237.86
116	113	690	C	14	X	4	55.0	56.0	238.25
74	113	690	C	14	X	4	86.0	87.0	238.56
114	113	690	C	14	X	5	17.0	18.0	239.37
112	113	690	C	14	X	5	74.0	75.0	239.94
54	113	690	C	14	X	5	128.0	129.0	240.48
81	113	690	C	15	X	1	33.0	34.0	243.23
3	113	690	C	15	X	1	81.0	82.0	243.71
91	113	690	C	15	X	1	136.0	137.0	244.26
104	113	690	C	15	X	2	19.5	20.5	244.60
67	113	690	C	15	X	2	82.0	83.0	245.22
82	113	690	C	15	X	2	130.0	131.0	245.70
83	113	690	C	15	X	3	14.0	15.0	246.04
46	113	690	C	15	X	3	48.0	49.0	246.38
105	113	690	C	15	X	3	56.5	57.5	246.47
70	113	690	C	15	X	3	83.0	84.0	246.73
42	113	690	C	15	X	3	102.5	103.5	246.93
41	113	690	C	15	X	3	108.0	109.0	246.98
63	113	690	C	15	X	3	140.5	141.5	247.31
1	113	690	C	15	X	4	18.0	19.0	247.58
9	113	690	C	15	X	4	30.0	31.0	247.70
50	113	690	C	15	X	4	47.5	48.5	247.88
121	113	690	C	15	X	4	56.0	57.0	247.96
31	113	690	C	15	X	4	68.5	70.0	248.09
113	113	690	C	15	X	4	79.0	80.0	248.19
55	113	690	C	15	X	4	93.0	94.0	248.33
30	113	690	C	15	X	4	105.5	107.0	248.46
60	113	690	C	15	X	4	116.5	117.5	248.57
33	113	690	C	15	X	4	126.0	127.5	248.66
76	113	690	C	15	X	4	136.0	137.0	248.76
4	113	690	C	15	X	4	144.0	145.0	248.84
90	113	690	C	16	X	1	22.0	23.0	252.72
101	113	690	C	16	X	1	83.0	84.0	253.33
115	113	690	C	16	X	1	128.0	129.0	253.78
7	113	690	C	16	X	2	30.0	31.0	254.30
89	113	690	C	16	X	2	78.5	79.5	254.79

Sample Vial #	Leg	Site	Hole	Core	Type	Section	Top(cm)	Bot(cm)	Depth(mbsf)
18	113	690	C	16	X	2	123.0	125.0	255.23
109	113	690	C	16	X	3	19.0	20.0	255.69
84	113	690	C	16	X	3	74.0	75.0	256.24
52	113	690	C	16	X	3	134.0	135.0	256.84
78	113	690	C	16	X	4	14.0	15.5	257.14
59	113	690	C	16	X	4	29.0	30.0	257.29
71	113	690	C	16	X	4	62.0	63.0	257.62
26	113	690	C	16	X	CC	26.0	27.0	258.16
21	113	690	C	17	X	1	146.0	147.0	263.26
27	113	690	C	17	X	2	8.0	9.0	263.38
94	113	690	C	17	X	2	87.5	89.0	264.18
53	113	690	C	17	X	3	27.0	28.0	265.07
40	113	690	C	17	X	3	82.0	83.0	265.62
43	113	690	C	17	X	3	136.0	137.0	266.16
6	113	690	C	17	X	4	5.0	6.5	266.35
12	113	690	C	17	X	CC	23.0	24.0	266.74
85	113	690	C	18	X	1	35.0	36.0	271.75
108	113	690	C	18	X	1	105.5	106.5	272.46
103	113	690	C	18	X	2	23.0	24.0	273.13
97	113	690	C	18	X	2	106.0	107.0	273.96
120	113	690	C	18	X	3	46.0	47.0	274.86
45	113	690	C	18	X	3	127.0	128.0	275.67
110	113	690	C	18	X	4	39.0	40.0	276.29
99	113	690	C	18	X	4	123.5	124.5	277.14
15	113	690	C	18	X	5	9.0	10.0	277.49
124	113	690	C	18	X	5	56.0	57.0	277.96

Appendix B

Ocean Drilling Program Sample Type and Quality Notes (1 = Yes, 0 = No, Appendix A for Vial # Correlation)

Sample Vial #	Depth (mbsf)	Plug	Loose Plug	Affixed Chunk	Chunk	Disturbed Chunk	Mold	Moist
65	192.01	0	0	0	1	0	0	1
16	193.48	0	0	0	1	0	0	1
19	195.01	0	0	0	1	0	0	1
87	196.53	0	0	0	1	0	0	0
106	197.73	0	0	0	1	0	0	0
62	199.00	0	0	0	0	0	0	0
68	200.51	1	0	0	0	0	0	0
95	202.01	0	0	0	1	0	0	0
44	203.52	1	0	0	1	0	0	0
73	205.58	1	0	0	1	0	0	0
80	206.52	1	0	0	1	0	0	0
17	207.99	0	0	0	1	0	0	0
22	209.49	0	0	0	1	0	0	0
10	210.78	0	0	0	1	0	0	0
111	212.67	0	0	0	0	0	0	0
56	215.31	0	0	0	0	0	0	0
28	215.83	0	0	0	1	0	0	0
100	224.09	1	0	0	0	0	0	0
118	224.64	1	0	0	0	0	0	0
29	225.73	1	0	0	0	0	0	0
117	226.31	1	0	0	0	0	0	0
66	227.16	1	0	0	0	0	0	0
2	227.84	1	0	0	0	0	0	0
34	228.67	0	0	0	0	0	0	0
77	229.50	0	0	0	0	0	0	0
47	230.06	1	0	0	0	0	0	0
58	230.85	1	0	0	0	0	0	0
51	231.25	1	0	0	0	0	0	0
98	232.06	1	0	0	0	0	0	0
107	233.45	1	0	0	0	0	0	0
123	233.92	1	0	0	1	0	0	0
37	234.56	1	0	0	0	0	0	1
93	234.81	1	0	0	0	0	0	0
122	235.55	1	0	0	0	0	0	0
8	236.09	1	0	0	0	0	0	0
11	236.40	1	0	0	0	0	0	0

Sample Vial #	Depth (mbsf)	Plug	Loose Plug	Affixed Chunk	Chunk	Disturbed Chunk	Mold	Moist
79	237.01	1	0	0	0	0	1	0
86	237.60	1	0	0	0	0	0	0
88	237.86	1	0	0	0	0	0	0
116	238.25	1	0	0	0	0	0	0
74	238.56	1	0	0	0	0	0	0
114	239.37	1	0	0	0	0	0	0
112	239.94	1	0	0	0	0	0	0
54	240.48	1	0	0	0	0	0	0
81	243.23	1	0	0	0	1	0	0
3	243.71	0	0	0	0	0	0	0
91	244.26	0	0	0	0	0	0	0
104	244.60	1	0	0	0	0	0	0
67	245.22	1	0	0	0	0	0	0
82	245.70	0	0	0	0	0	0	0
83	246.04	1	0	0	0	0	0	0
25	246.21	0	0	0	1	0	0	0
46	246.38	1	0	0	0	0	0	0
105	246.47	1	0	0	0	0	0	0
70	246.73	1	0	0	0	0	0	0
42	246.93	1	0	0	0	0	0	0
41	246.98	1	0	0	0	0	0	0
63	247.31	0	0	0	1	0	0	0
1	247.58	0	0	0	1	0	0	0
9	247.70	0	0	0	1	0	0	0
50	247.88	0	0	1	0	0	0	0
121	247.96	0	0	0	1	0	0	0
31	248.09	0	0	0	1	0	0	0
113	248.19	0	0	0	0	0	0	0
55	248.33	1	0	0	0	0	0	0
30	248.46	0	0	0	1	0	0	0
60	248.57	1	0	0	0	0	0	0
33	248.66	0	0	0	1	0	0	0
76	248.76	1	0	0	0	0	0	0
4	248.84	0	0	0	1	0	0	0
90	252.72	0	0	0	1	0	0	0
101	253.33	1	0	0	0	0	0	0
115	253.78	0	0	0	0	0	0	0
7	254.30	1	0	0	0	0	0	0
89	254.79	0	0	0	1	0	0	0
18	255.23	0	0	0	1	0	0	0
109	255.69	0	0	0	1	0	0	0

Sample Vial #	Depth (mbsf)	Plug	Loose Plug	Affixed Chunk	Chunk	Disturbed Chunk	Mold	Moist
84	256.24	1	0	0	0	0	0	0
52	256.84	1	0	0	0	0	0	0
78	257.14	0	0	0	1	0	0	0
59	257.29	1	0	0	0	0	0	0
71	257.62	1	0	0	0	0	0	0
26	258.16	0	0	0	0	0	0	0
119	262.03	1	0	0	0	0	0	0
14	262.69	1	0	0	0	0	0	0
21	263.26	1	0	0	0	0	0	0
27	263.38	0	0	0	1	0	0	0
94	264.18	0	0	0	1	0	0	0
53	265.07	1	0	0	0	0	0	0
40	265.62	1	0	0	0	0	0	0
43	266.16	0	0	0	1	0	0	0
6	266.35	0	0	0	1	1	0	0
12	266.74	0	0	0	0	0	0	0
85	271.75	1	0	0	0	0	0	0
108	272.46	1	0	0	0	0	0	1
103	273.13	1	0	0	0	0	0	1
97	273.96	1	0	0	0	0	0	1
120	274.86	1	0	0	0	0	0	1
45	275.67	1	0	0	0	0	0	1
110	276.29	1	0	0	0	0	0	1
99	277.14	1	0	0	0	0	0	0
15	277.49	0	0	0	1	0	0	0
124	277.96	0	0	0	1	1	0	0

Appendix C

Compiled Data for Results and Discussion Sections

Sample Vial	Depth(mbsf)	$\delta^{15}N_{decarb}$(‰)	$\delta^{13}C_{org(decarb)}$(‰)	Elemental N_{decarb}(%)	Elemental C_{decarb}(%)
65	192.01	4.4	-25.9	0.03	0.19
16	193.48	4.9	-26.5	0.02	0.24
19	195.01	4.4	-27.0	0.02	0.20
87	196.53	6.8	-26.7	0.03	0.25
106	197.73	8.8	-26.3	0.01	0.10
62	199.00	4.7	-25.8	0.03	0.25
68	200.51	4.1	-26.0	0.02	0.20
95	202.01	5.0	-26.3	0.02	0.18
44	203.52	4.2	-27.0	0.02	0.25
73	205.58	5.5	-26.5	0.02	0.10
80	206.52	8.2	-26.8	0.03	0.24
17	207.99	4.6	-27.7	0.02	0.29
22	209.49	3.0	-27.2	0.02	0.23
10	210.78	3.4	-27.4	0.02	0.17
111	212.67	8.8	-26.7	0.02	0.22
28	215.83	2.1	-26.5	0.01	0.24
100	224.09	5.6	-27.3	0.02	0.12
118	224.64	9.5	-26.4	0.02	0.21
29	225.73	4.1	-26.2	0.01	0.20
117	226.31	9.0	-26.8	0.02	0.15
66	227.16	4.2	-33.5	0.02	0.19
2	227.84	2.7	-25.8	0.01	0.16
34	228.67	3.6	-27.0	0.01	0.14
77	229.50	8.5	-32.7	0.02	0.18
47	230.06	12.6	-26.8	0.01	0.15
58	230.85	8.1	-27.1	0.01	0.12
51	231.25	11.8	-26.8	N/A	0.11
98	232.06	5.7	-28.9	0.01	0.09
107	233.45	11.4	-30.9	0.01	0.12
123	233.92	3.6	-26.7	0.01	0.17
37	234.56	1.4	-26.5	0.01	0.09
93	234.81	3.4	-26.5	0.01	0.07
122	235.55	5.2	-26.6	0.01	0.15
8	236.09	2.0	-25.8	0.01	0.16
11	236.40	1.5	-26.0	0.01	0.19
79	237.01	9.7	-27.1	0.01	0.13
86	237.60	11.0	-27.9	0.01	0.12
88	237.86	9.7	-26.3	0.01	0.14

Sample Vial	Depth(mbsf)	$\delta^{15}N_{decarb}$(‰)	$\delta^{13}C_{org(decarb)}$(‰)	Elemental N_{decarb}(%)	Elemental C_{decarb}(%)
116	238.25	8.2	-26.3	0.01	0.20
74	238.56	5.8	-26.8	0.01	0.16
114	239.37	9.8	-29.7	0.01	0.10
112	239.94	10.4	-26.7	0.01	0.17
54	240.48	8.6	-28.7	0.01	N/A
81	243.23	9.2	-27.4	0.01	N/A
3	243.71	2.7	-26.5	0.01	0.18
91	244.26	5.3	-26.1	0.01	0.16
104	244.60	5.4	-26.7	0.01	0.11
67	245.22	4.1	-25.5	0.01	0.16
82	245.70	8.7	-26.3	0.01	0.10
83	246.04	11.5	-26.2	0.01	0.12
46	246.38	10.7	-32.4	0.01	0.16
105	246.47	11.4	-26.5	0.01	0.08
70	246.73	4.2	-27.7	0.01	0.18
42	246.93	3.1	-26.4	0.01	0.06
41	246.98	3.5	-26.8	0.01	0.06
63	247.31	3.7	-26.4	0.01	0.05
1	247.58	2.4	-26.3	0.01	0.11
9	247.70	2.5	-26.0	0.01	0.07
50	247.88	12.0	-25.8	0.01	0.10
121	247.96	3.8	-26.4	0.01	0.13
31	248.09	2.4	-26.6	0.02	0.10
113	248.19	7.2	-26.4	0.02	0.20
55	248.33	7.9	-26.5	0.02	0.16
30	248.46	3.2	-26.4	0.01	0.20
60	248.57	7.3	-26.3	0.01	0.10
33	248.66	3.7	-26.3	0.02	0.16
76	248.76	8.1	-25.6	0.02	0.18
4	248.84	3.0	-26.0	0.02	0.14
90	252.72	9.5	-27.0	0.02	0.24
101	253.33	5.2	-26.8	0.02	0.19
115	253.78	6.8	-26.6	0.02	0.19
7	254.30	4.1	-26.6	0.02	0.13
89	254.79	8.6	-27.4	0.02	0.19
18	255.23	3.5	-27.3	0.02	0.22
109	255.69	9.6	-27.1	0.02	0.26
84	256.24	9.8	-30.3	0.02	0.24
52	256.84	8.6	-26.5	0.01	0.11
78	257.14	7.7	-26.5	0.02	0.19
59	257.29	6.4	-32.7	0.02	0.27

Sample Vial	Depth(mbsf)	$\delta^{15}N_{decarb}$(‰)	$\delta^{13}C_{org(decarb)}$(‰)	Elemental N_{decarb}(%)	Elemental C_{decarb}(%)
71	257.62	4.8	-26.2	0.02	0.14
26	258.16	4.4	-27.1	0.02	0.13
21	263.26	5.5	-25.2	0.02	0.10
27	263.38	3.7	-27.3	0.02	0.15
94	264.18	6.8	-27.6	0.02	0.15
53	265.07	8.5	-26.5	0.01	0.16
40	265.62	4.0	-26.6	0.03	0.19
43	266.16	4.3	-27.3	0.02	0.15
6	266.35	4.5	-27.2	0.03	0.14
12	266.74	5.0	-26.7	0.02	0.16
85	271.75	8.5	-27.4	0.02	0.21
108	272.46	8.7	-26.6	0.03	0.26
103	273.13	6.7	-27.0	0.02	0.16
97	273.96	5.9	-27.3	0.02	0.10
120	274.86	8.7	-28.6	0.02	0.10
45	275.67	7.2	-26.9	0.02	0.18
110	276.29	9.7	-26.5	0.02	0.28
99	277.14	5.7	-27.0	0.02	0.11
15	277.49	5.0	-27.1	0.02	0.31
124	277.96	7.3	-27.7	0.02	0.17

VITA

Bradley Alan Beckwith

Candidate for the Degree of

Master of Science

Thesis: THE MARINE NITROGEN CYCLE ACROSS THE CRETACEOUS-PALEOGENE BOUNARY AT MAUD RISE

Major Field: GEOLOGY

Biographical:

Education:

Completed the requirements for the Master of Science in Geology at Oklahoma State University, Stillwater, Oklahoma in July, 2016

Completed the requirements for the Bachelor of Science in Geosciences at Texas Tech University, Lubbock, Texas in August, 2013

Experience:

Mud Logger
Teaching Assistant
Petroleum Geologist Intern
Research Assistant
2nd Year Plumber's Apprentice
Landscaping Foreman
Construction Laborer

Professional Memberships:

Oklahoma City Geological Society
Tulsa Geological Society
American Association of Petroleum Geologists